CONTENT
Vol. 6. No. 3-2020

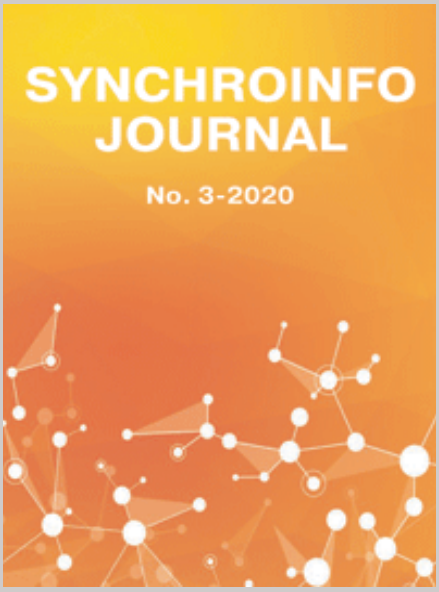

Published bi-monthly since 2015.

ISSN 2664-066X (Print)
ISSN 2664-0678 (Online)

Publisher
Institute of Radio and Information Systems (IRIS), Vienna, Austria

Address:
1010 Wien, Austria,
Ebendorferstrasse 10/6b
media-publisher.eu/
synchroinfo-journal

METHODOLOGY FOR THE ORGANIZATION AND DESIGN OF DISPATCH SERVICES

Kulpunai A. Adylbekova
Kyrgyz State Technical University, Bishkek

Mohammed Omar Ahmed Abdulwasea
Sana'a University, Sana, Republic of Yemen

DOI: 10.36724/2664-066X-2020-6-3-2-4

ABSTRACT

Security and stable socio-economic development of any country depends on the effectiveness of the mechanism for prompt response to emerging threats. Complex of software and hardware "System 112" is designed for automated processing of emergency calls to a single number "112". The design of unified dispatch services (UDS) allows to apply theoretical knowledge to solve urgent practical problems. It is proposed to design the UDS service for mastering the competencies of the educational standard in two stages. Namely, to make preliminary planning and preliminary estimation of the amount of equipment required to deploy the service. Further, the performance indicators of the UDS are evaluated, taking into account the possibility of routing part of the traffic to the dedicated emergency services.

KEYWORDS: *Unified dispatching service, emergency services, call service center, prompt response, special software.*

I. INTRODUCTION

Concern for the life and health of citizens, the safety of property, ensuring personal and public safety, as well as the need to counter man-made, natural threats and acts of terrorism require the development of a mechanism for a rapid response to threats. As a single emergency call number in the Russian Federation, 112 was assigned, which combined four emergency services (fire brigade, police, ambulance and gas network emergency service) and two new services (Anti-terror and emergency response service).

Introduction

System 112 – multifunctional information and communication geographically distributed automated information and control system created within the boundaries of the subject [1, 2, 3, 4].

The block diagram of system 112 is shown in Figure 1.

It consists of different subsystems providing functions such as:

– receiving and processing calls;
– da abase;
– decision support;
– geo nformation subsystem;
– onitoring;
– raining;
– technological support;
– fixed communication, data transmission and radio communication;
– information security subsystem.

Analysis of the deployment and operation of System 112 in the pilot regions showed that the most important in terms of organizing information interaction of departmental dispatch services is the subsystem for receiving and processing calls (messages about incidents) coming to the unified dispatch service. The specified subsystem includes a call service center (CSC). The subsystem for receiving and processing calls, or the so-called dispatch subsystem (DS), is a control subsystem in the automated system (AS) of the Unified Dispatch Service (UDS).

Currently, several software and hardware options for building this subsystem are possible from the point of view of organizing interagency cooperation. Let's consider two of the most common options.

Option 1. The emergency services DDS (01, 02, 03) already have their own departmental dispatch systems. Special software (SS) for call processing should be created for the call processing center (CPC) based on the UDDS and for the DS of the emergency operational service, geographically corresponding to the UDS. In practice, this can be implemented by placing a remote client workstation in the DS with the open source software for the call center of the UDS in addition to the departmental AWP for receiving messages about incidents or the development of a special integration software module to ensure information interaction of the open source call center of the call center with the special software for the emergency services.

Option 2. Development of unified automated system of operational dispatch control in each of tDDS separately and as a whole. A unified system should ensure the principle of entering data through one application only once, data should be available for other applications without copying it. All actions of the operator (dispatcher) in the system should be automatically recorded in real time with saving information by whom this action was carried out and when, so that the incident and actions of emergency services personnel on it could be fully restored, including for training goals.

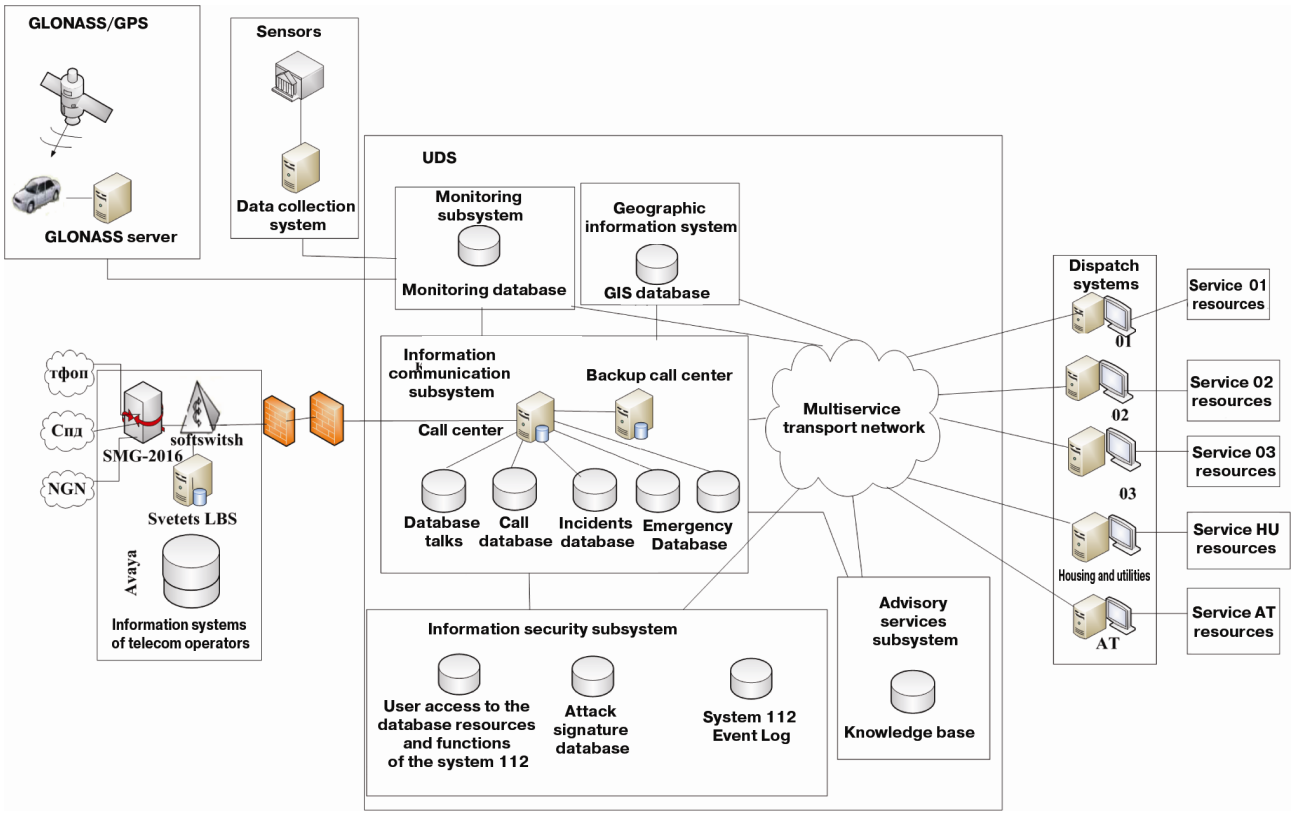

Figure 1. Block diagram of system-112

Each option has the right to exist and can be implemented in a particular subject. The second option is more preferable, which is more complicated at the initial stage, but later, when the system is replicated in the regions, the implementation effect levels out the problems that arose during development.

As an example of open source software development, we present data for specialized software based on "ISTOK-CM". This is a unique system of instant information exchange and group work, response services of different departmental affiliations, capable of reaching hundreds of organizations – participants involved in emergency and rescue operations and providing prompt decision-making based on the latest reports. The introduction of a standard solution based on the open source software "ISTOK-SM" in UDS and DS of emergency response allows making decisions faster, as it accelerates the collection, processing and distribution of information in all interaction services at all levels.

The Call Service Center (CSC) is an important component of the "System 112", which ensures the reception of calls from the population of the administrative center of the subject and their transfer for service to interacting EDDS, centralized data storage, interaction with the regional navigation and information center of the emergency response system (ERA-GLONASS).

Such call center functions can be implemented on the basis of Avaya Aura Communication Manager (ACM), which, along with calls from landline and mobile telephones, can handle e-mail messages, SMS (which may be more convenient for people with disabilities) and video calls. In the case of an interrupted call, the connection can be automatically restored (Call Back Assist). The development strategy of the solution provides for its integration with applications for smartphones, tablets and with social networks as alternative channels of interaction.

Another current Avaya development is the Avaya Notification Solution (ANS). It is able to provide notification of large groups of the population about an emergency situation through all channels: voice communication (city telephone network, wireless, departmental networks), SMS, e-mail, chats, IP phones, speakers, loudspeakers, text messages on the display phone.

This solution is scalable, highly reliable and can work with equipment from other manufacturers. ANS is currently being implemented, for example, in Netherlands.

To ensure the reliability of the system, a backup call center (BCC) is installed. When the call center fails in the system, the transition to the radio call center is performed in stages [5, 6]:

– at he first stage, the call processing is carried out by the duty shift and employees of the BCC admitted to duty, including from among the trainees;

– at the second stage, the staff on duty of the call centers arriving for reinforcement are connected to call processing.

Let us also consider the possibilities of ECSS-10 – a complex solution for building an emergency call service center "System 112" based on the ECSS-10 Softswitch. The hardware and software complex is a combination of software and hardware components developed in Russia, providing a high level of reliability and protection from the presence of "bugs" in the program code.

It is designed to unify the interface of interaction between telecom operators and the call service center of System 112. Telecom operators can connect to UOVEOS using E1 streams (OKS-7) and VoIP protocols SIP, SIP-T, SIP-I. The SIP protocol is used as the interface for interaction between UOVEOS and the System 112 call center.

The ECSS-10 UO-VEOS hardware and software complex consists of the following components:

– program switch ECSS-10 Softswitch;

– trunk gateways SMG-1016M and SMG-2016;

– SBC-1000 and SBC-2000 session border controllers;

– location server TSMN Svetets LBS;

– unified management and monitoring system Eltex EMS.

The general scheme of the "System 112" operation is shown in Figure 2, as an example of a solution by Ericsson Coordcom. The number of dispatchers is variable, as is number of connected response services.

The process of operation of System 112 will be organized in the following way: a message about an incident is received at the call service center 112, or at the DS of one of the emergency services included in System 112. Further, in an automated mode, the operator enters the main characteristics of the incident into the database, transfers them to the DS for the intended purpose, monitors the response to the incident, analyzes and enters the information obtained as a result of the response into the database, if necessary clarifies and corrects the actions of involved DS and informs the interacting DS about operational situation, measures taken and implemented. During and after the end of measures for emergency response to a received call or message, the DS must enter information on the measures taken into the System 112 database.

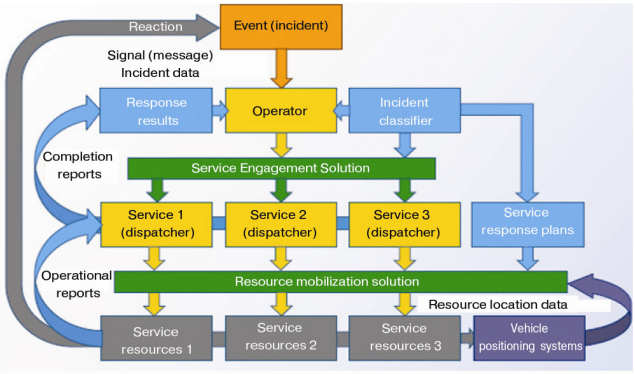

Figure 2. General scheme of emergency response

References

1. Order of the Government of the Russian Federation of August 25, 2008 No. 1240-r on the approval of the Concept for the creation of System-112.

2. GOST R22. 7.01-99 UDS. Basic provisions.

3. https://www.osp.ru/lan/2012/10/13017656/ (25.11.2019).

4. http://www.myshared.ru/slide/395795/ (25.11.2019).

5. http://www.secuteck.ru/articles2/firesec/sistema-112-ot-potrebnostey- k- realizatsii/ (23.11.2019).

6. https://eltexsl.ru/uoveos-solutions/ (25.11.2019).

7. https://nag.ru/articles/article/21574/u-sistem-spaseniya-slojnoe-buduschee.html (20.11.2019).

SYNTHESIS OF STRUCTURAL ELECTRICAL CIRCUITS OF RADIO ENGINEERING DEVICES IN A HYBRID PRODUCTION EXPERT SYSTEM

Georgy A. Dolin, Anastasiya Y. Kudryashova,
Moscow Technical University of Communications and Informatics, Moscow, Russia,
dolin1974@gmail.com, asykka@bk.ru

DOI: 10.36724/2664-066X-2020-6-2-5-9

ABSTRACT

The development of communication systems and devices requires full automation of their design process to quickly update the RED. Especially important is the development of software for the synthesis of basic electrical circuits. The article describes the algorithm of end-to-end CAD based on an expert system for the synthesis of basic electrical circuits of RED based on an object-oriented hybrid expert system. Algorithms for forming the knowledge base at the learning stage and output in the synthesis process are considered. The algorithmic and software hybrid production ES and knowledge base are described. The system organization of structured information about the synthesis of blocks and the entire RED. It allows you to effectively form and manipulate the knowledge of RED design experts. The method for introducing and using a set of constant and variable confidence coefficients in the ES has been developed, which allows using unformalized knowledge about the field of RTU design. This ensures the application of both the knowledge obtained during the training of the ES and the knowledge accumulated during the design of the RED of the ES itself. All this allows the designer to formalize knowledge faster and more accurately, as well as increase the speed of automatic design since unlikely circuit solutions are not considered.

KEYWORDS: *expert system, Radio Technical Devices, CAD, knowledge base, algorithmic structures*

INTRODUCTION

Analysis of the accumulated experience in the field of Radio Engineering Devices (RED) design automation has shown that it is possible to ensure the synthesis and modeling of RED of any structure with a high degree of reliability and optimality only by creating a CAD system containing an ES that allows you to present and programmatically implement empirical knowledge, as well as heuristic rules and techniques used by highly qualified specialists in the design of RED in traditional manual design [1].

Expert synthesis allows you to provide a lack of a priori information with greater unambiguity and reliability of decisions made during automatic structural synthesis of RED in CAD and the accumulation of design experience of qualified RED design experts. It allows unskilled or novice users to design RED at the level of expert designers by formalizing the collective knowledge of a group of highly qualified experts about the field of RED design.

ES are classified according to the following set of characteristics: purpose; stage of existence; type of PS; type of knowledge representation methods used; universality; basic properties; operating environment. For automated RED synthesis in CAD, it is advisable to develop an ES of the following type: by purpose – research; by type-developed in algorithmic programming languages; by the type of knowledge representation methods used - hybrid, combining symbolic representation of knowledge with mathematical calculations necessary for the design of RED and allowing the use of data stored in external databases in ES; by the type of universality of knowledge representation - with an integral representation, combining several models of knowledge representation; operating in Windows operating systems on a PC.

I. The advantages of ES

ES are designed for solving so-called weakly formalized or unformalized tasks. According to [2], unformalized tasks include those that have one or more of the following characteristics: tasks cannot be set in numerical form; goals cannot be expressed in terms of a precisely defined target function; there is no single target function in the design of RTU, and often for individual nodes; there is no algorithmic solution to problems; the customer does not have complete source information and reliable units of measurement for some parameters; an algorithmic solution exists, but it cannot be used due to limited resources (time, memory, etc.); the amount of source information and data is very large, variable, and requires a significant amount of time for familiarization, which leads to the need to reduce the search space to reduce the design time. ES are used to solve difficult practical problems, which include circuit synthesis of RTU. In terms of quality and efficiency of solutions, such ES are not inferior to the solutions of a human expert, and often surpass them [5] due to the accumulation of knowledge of a group of expert designers and reducing the subjectivity of their decisions. The output process in the ES has clarity, i.e. solutions can be explained to the user at a qualitative level (in contrast to solutions obtained using numerical algorithms and from solutions obtained by statistical methods).

This quality of ES is provided by their ability to reason about their knowledge and conclusions. They can add to their knowledge both in the course of interaction with an expert, and with a novice user in the constructive or non-constructive solution of the problem.

Let's note further the advantages of ES over a human expert:

- ES has no preconceptions;
- ES don't jump to conclusions;
- ES work in a systematic way, considering all the details, often choosing the best alternative from all possible ones.

KB ES can be exceptionally large. Once entered the machine, knowledge is stored forever. A person has a limited KB, and if the data is not used for a long time, they are forgotten and lost forever.

Like other types of computer programs, ES cannot replace a person in solving problems, but rather represent a special kind of tools that allow them to solve problems faster and more efficiently. In addition, knowledge-based systems can be viewed by users as a form of replication - a new way to record and disseminate knowledge.

Therefore, it is possible to provide automatic circuit synthesis and subsequent modeling of RED of any structure only by developing a CAD system containing ES, which will allow forming and storing empirical knowledge used by specialists in the design of RED in traditional manual or automated design, as well as synthesizing constructive RED due to a priori exclusion by design experts of unrealizable and little-promising RED nodes from the KB ES [1].

Selected due to several advantages, the hybrid production ES includes the following main blocks: the KB, the output machine, and the user interface. KB ES consists of facts and rules.

The KB facts describe what is known about the RED synthesis technique now. In the KB of a production ES, facts are represented as a triple: object-attribute-value. The object in RED synthesis is the technical parameters or characteristics of the device that is assigned a value, and the attribute – determines the confidence coefficient for the object value. In KB, rules form a certain hierarchy, which can be represented as a graph consisting of vertices and edges. Each vertex corresponds to an object that has certain values. Each edge is defined by a pair of vertices and corresponds to one of the possible ways to reach the goal. A graph can be represented as a tree whose branches correspond to the edges of the graph, and whose nodes correspond to the vertices of the graph.

There are two groups of requirements for knowledge representation methods for designing RED [2, 5]. the Requirements of the first group of knowledge representation methods assume the following: universality, integrity, and openness of knowledge representation. This group of requirements contributes to improving the efficiency and obtaining high performance characteristics of the developed RED [4]. The second group of methods regulates the functionality of the RED and is crucial for the practical use of CAD. The requirements of the second group imply ensuring the following factors: the adequacy of the display of the subject area, i.e. such a description that can simulate any processes occurring in this subject area and essential for the selected class of problems; the natural form of the description of the subject area in the knowledge system, which allows you to create a human-friendly interface with the computer system in the process of setting and solving design problems [6]; multilevel or hierarchical description of the subject area, which provides solutions to complex design problems; a combination of procedural and declarative methods in a single knowledge system that allows, on the one hand, to simply describe the basic concepts and terminology of the subject area, and on the other - to set functional dependencies and formal [7].

For the synthesis of RED structural schemes, it is advisable to use the production model of knowledge representation about RED, since in the production ES, the conclusion is made in the opposite direction from the statements that must be proved, which significantly speeds up the result; modularity of the rules organization; independence of rules that Express separate unrelated fragments of knowledge; separation of control knowledge from subject knowledge, which allows you to apply various control strategies, including using statistics, for example, the Bayes full probability formula; the ability to create control mechanisms for automatic design of RED. At the same time, the hybrid production ES includes the following main blocks: the knowledge base (KB), the output machine, and the user interface. KB ES consists of facts, questions, and rules.

The KB facts describe what is known about the method of RED synthesis at this moment. In the KB of a production ES, facts are represented as a triple: object-attribute-value. The object in RED synthesis is the technical parameters or characteristics of the device that is assigned a value, and the attribute – determines the confidence coefficient for the object value. In KB, rules form a certain hierarchy, which can be represented as a graph consisting of vertices and edges. Each vertex corresponds to an object that has certain values. Each edge is defined by a pair of vertices and corresponds to one of the possible ways to reach the goal. A graph can be represented as a tree whose branches correspond to the edges of the graph, and whose nodes correspond to the vertices of the graph [2].

The rules in the KB of production ES using the language of representation of algorithmic structures are formulated in the following form:

< rule > :: = IF < premise > then < conclusion >;

< premise > :: = < triple > | < triple > And < premise >;

< triple > :: = < object > < logical operator> < value >, < attribute >;

< conclusion> :: = < three > | <action > | < three > And < conclusion >.

The rule is written as a conditional statement that includes a premise and conclusion. The premise may consist of one or more triples connected by the unions "And". the Conclusion may consist of one or more triples involving one or more actions. An action consists of one of four procedures: calculating a mathematical function, searching the database for an electronic component, saving an intermediate design result, or clearing the object value. An es output machine (rule interpreter) is an ES program block that implements the output process based on a DB and a working set (a part of memory allocated for storing rules and fact values during the output process).

The output machine performs two functions: first, viewing existing facts and rules from the database and adding new facts, and second, determining the order in which the rules are viewed and applied. The output machine performs the design process using rules, stores information about the conclusions obtained for the user, and requests information from him when there is not enough knowledge in the database to perform the next rule.

The RED design process in ES is a sequence of steps, each of which selects a rule from the KB that is used to determine the goal value. The process ends when the fact value is determined or it is shown that it cannot be determined. RED design can be performed in several ways [1], of which the most common are direct output order and reverse output order (depth-first search).

The direct order of inference is made from the facts that are in the working set to the conclusion. If such a conclusion can be found, it is entered in the working set.

In the full iteration method, vertexes are expanded in the order in which they are constructed. A simple tree iteration algorithm consists of the following sequence of steps:

1) Put the vertex in a list called OPEN.

2) If the list is OPEN and empty, the output is signaled that the search failed, otherwise proceed to the next step.

3) ke the first vertex from the OPEN list and move it to the CLOSED list; let's call this vertex n.

4) xpand the vertex n, forming all the vertices immediately following n. If there are no immediately following vertexes, then proceed immediately to step (2). Place the existing vertexes immediately following n at the end of the list of points AND build pointers leading from them back to vertex n.

5) If any of these immediately following n vertices are target vertices, then output the solution obtained by looking along the pointers; otherwise, proceed to step (2).

This algorithm assumes that the initial vertex does not meet the goal, although it is not difficult to enter a step to check this possibility. The vertices and pointers constructed during the iteration process form a subtree of the entire implicitly defined tree of the state space [8]. We will call such a subtree a brute force tree.

The full search method will certainly find the shortest path to the target vertex, provided that such a path exists at all. (If there is no such path, the specified method will declare failure in the case of finite graphs, and in the case of infinite graphs, the algorithm will never finish its work).

There may be problems in which the solution has some other requirements than the requirement to obtain the shortest sequence of operators. Assigning certain prices to tree arcs (followed by finding a decision path that has a minimum cost) meets many of these promised criteria. A more General version of the full search method, called the equal price method, allows you to find in all cases some path from the initial vertex to the target, the cost of which is minimal. While the algorithm described above propagates lines of equal path length from the starting vertex, the more General algorithm described below propagates lines of equal path cost. It is assumed that we are given a cost function c(ni, nj), which gives the cost of moving from a vertex ni to some next vertex nj. In the equal price method, for each vertex n in the iteration tree, we need to remember the cost of the path built from the initial vertex s to the vertex n. Let g(n) be the cost from vertex s to vertex n in the iteration tree. In the case of iteration trees, we can be sure that g(n) is also the cost of the path that has the minimum cost (since this path is the only one).

In the equal price method, vertices are revealed in ascending order of cost g(n). This method is characterized by the following sequence of steps:

1) Put the initial vertex s in a list called OPEN. Put g(s)=0.

2) If the list is OPEN and empty, the output is signaled that the search failed, otherwise proceed to the next step.

3) Take from the OPEN list the vertex for which the value of g has the smallest value, and put it in the CLOSED list. Give this vertex the name n. (If the values

match, choose the vertex with the minimum g at random, but always giving preference to the target vertex.)

4) f n is the target vertex, then output the decision path obtained by looking back in accordance with the pointers; otherwise, proceed to the next step.

5) xpand vertex n by constructing all the vertices immediately following it. If there are none, proceed to step (2). for each of these immediately next (child) vertices ni, calculate the cost of g(n) by putting g(ni)=g(n)+c(n,ni). Put these vertexes, along with their corresponding newly found values of n, in the list of points AND build pointers going back to T.

6) Go to step (2).

Checking whether a certain vertex is a target is included in this scheme so that minimal cost paths are guaranteed to be found.

An equal-price algorithm can also be used to find paths of minimal length if you simply put the cost of each edge equal to one. If there are several initial vertexes, and the algorithm is simply modified: in step (1), all initial vertexes are placed in the OPEN list. If the States that meet the goal can be described explicitly, then the iteration process can be started in the opposite direction, taking the target vertices as the initial ones and using the appeal of the operator G.

In depth-first search methods, the vertexes that were built last are revealed. Let's define the depth of the tree vertex as follows:

- The root depth of the tree is zero.
- The depth of any subsequent vertex is equal to one plus the depth of the vertex that immediately precedes it.
- Thus, the vertex that has the greatest depth in the search tree is currently the one that should be expanded at this moment.

This approach can lead to a process unfolding along some useless path, so you need to introduce some return procedure. After the process builds a vertex with a depth greater than a certain boundary depth, we reveal the vertices of the greatest depth that does not exceed this boundary, and so on.

The depth-first method is determined by the following sequence of steps:

1) Put the starting vertex in a list called OPEN.

2) If the list is OPEN and empty, the output is signaled that the search failed, otherwise go to step (3).

3) ke the first vertex from the OPEN list and move it to the CLOSED list. Give this vertex the name n.

4) If the depth of the vertex n is equal to the boundary depth, then go to (2), otherwise to (5).

5) xpand vertex n by constructing all the vertices immediately following it. Put them (in any order) at the beginning of the list of OBJECTS and build pointers going from them to n.

6) If one of these vertexes is a target, then output the solution by looking at the corresponding pointers, otherwise go to step (2).

The depth - first search algorithm iterates along one path until the maximum depth is reached, then considers alternative paths of the same or lower depth that differ from it only by the last step, then considers paths marked by the last two steps, and so on.

II. The purpose of the ES

The purpose of the ES is to determine the value of the object specified by the designer, or to make sure that with this level of knowledge IN the ES database, the object value cannot be determined. The value of an object can either be pre-defined in the KB of the ES, or it is extracted by the ES from the dialog with the designer [3].

The RED design process in ES is a sequence of steps, each of which selects a rule from the KB that is used to determine the goal value. The process ends when the fact value is determined, or it is shown that it cannot be determined. RED design can be performed in several ways, the most common of which are direct output order and reverse output order (depth - first search).

The direct order of inference is made from the facts that are in the working set to the conclusion. If such a conclusion can be found, it is entered in the working set. Depth-first search: rules are viewed until they are found in working memory or object values are received from the user that confirm one of the rule conclusions. Initially, the designer sets a goal-to determine the design object.

When searching in depth, the inference machine searches for a rule containing the design goal in the conclusion, and then in the process of working with the ES, the inference machine goes back, moving from conclusions to conditions, and tries to find among them those that confirm this proposal. If it turns out to be correct, then the next object is put forward, detailing the first one, which is a sub-goal in relation to it.

Next, we look for conditions that confirm the truth of the subordinate conclusion. Search in depth is used in cases where the goals are known and relatively few of them, which is most consistent with the method of synthesis of RED structural schemes. In addition, this method of achieving the goal allows you to speed up the design process by introducing confidence coefficients to select the further path of movement along the tree, i.e. reducing the search space in width, and taking into account the variance of confidence coefficients to reduce the search space in depth. Therefore, due to the noted analogies and advantages, this method of achieving the goal is chosen for the implementation of the process of synthesis of structural schemes of RED in ES [5].

To implement the circuit synthesis of RED in the output machine of the production ES, at least the following procedures should be implemented: FIND, SOLVE, SAVE, and CLEAN.

To find the required electronic components MOUTH on specified parameters to a procedure FIND (Query_SQL), you must pass the SQL query of the following form: choose all components from the database, where the values given by an expert or identified in the process output parameters of the required electronic components more or less equal to the values of the component parameters in the database.

The result of this procedure is the selection of electronic components whose parameters meet the constraints specified in the request. If the query results in multiple components, the designer is asked to select one of them, or the ES automatically selects the first appropriate one. To calculate the values of mathematical expressions that contain integers and decimals, parentheses, signs of four arithmetic operations, and mathematical functions such as exponentiation, root extraction, integration, differentiation, and so on, and are written as a string, you need to implement their parsing (the SOLVE/EXPRESSION procedure).

To do this, it is advisable to use the Polish form of writing (Backus notation) mathematical expressions. The SAVE (list of objects) procedure allows you to save the design results in a text file, and the CLEAR (object) procedure allows you to clear the object value defined during the design process.

The algorithm for synthesis of RED structural schemes in a hybrid production ES includes the following steps. The analysis of the TOR includes entering the parameters of the TOR by the designer and forming the design goal. If the designer does not have the values of the required parameters, the ES cannot carry out the design process. And if it is necessary to take into account additional requirements of the TOR, the designer should make changes to the KB ES. At this stage, the reliability of heuristic information stored in the database and necessary for constructive synthesis is of particular importance [4].

The development of the device at the structural level includes the selection of the nomenclature of nodes and cascades of the structural scheme of the designed RED from the KB. The hybrid production expert system allows you to present methods for the synthesis of RED structural schemes in the form of rules. They make it possible to save the conclusions obtained for the user and request additional information from him, calculate the required parameters of structural schemes based on functional relationships, and select electronic components based on several parameters from the database. The synthesis of structural schemes is carried out in a hybrid production ES that operates with symbolic information in combination with formula relations. Structural design ends with the formation of requirements for the parameters of individual RED nodes, which should ensure the operation of the entire device.

Conclusion

Thus, the hybrid production ES allows you to implement expert circuit synthesis of structural diagrams of individual nodes and the entire RED as a whole, due to the fact that the output process is similar to the process of reasoning of an expert designer. In addition, the ES provides the calculation of the required parameters of the RED block diagram by functional relationships and it is possible to select electronic components based on a set of parameters from the database. At the same time, the use of confidence coefficients for choosing the design direction and taking into account the variance of confidence coefficients allows you to speed up the design process by reducing the search space in depth and width.

References

1. G. A. Dolin, "Object-Oriented Representation of Mixed Models Knowledge in the Design of Electronic Devices in CAD Electra," *2020 Systems of Signals Generating and Processing in the Field of on Board Communications*, Moscow, Russia, 2020, pp. 1-5, doi: 10.1109/IEEECONF48371.2020.9078546.

2. G. . Dolin, "Using a distributed database of parameters of electronic components in course design," *Methodological issues of teaching infocommunications in higher school*, 2018. No 2. pp. 10-14.

3. G. A. Dolin, "Formation the knowledge base of red expert design for conducting coursework and lectures," *Methodological issues of teaching infocommunications in higher school*, 2018. No 2. pp. 46-53.

4. G. A. Dolin, "Circuit Analysis, Synthesis and Simulation of Radio Devices in Electra CAD," *2019 Systems of Signals Generating and Processing in the Field of on Board Communications*, Moscow, Russia, 2019, pp. 1-6, doi: 10.1109/SOSG.2019.8706814.

5. G. A. Dolin "Automation of synthesis of structural and basic electrical circuits of RED in production and object-oriented expert systems," *2018 Actual problems of radio and film technologies. II all-Russian scientific and technical conference*. Saint Petersburg, Saint Petersburg state Institute of film and television, October 24-27, 2018. Collection of works. pp. 40-45

6. K. V. Boychenko, J. Rivory, I. V. Boychenko, A.Y. Kudryashova, "Interactive Space as a Signal Processing Device," *2020 Systems of Signal Synchronization, Generating and Processing in Telecommunications (SYNCHROINFO)*, Svetlogorsk, Russia, 2020, pp. 1-10.1109/SYNCHROINFO49631.2020.9166033.

7. K. V. Boychenko , I. V. Boychenko, A.Y. Kudryashova, "Interactive built environment in shaping users orientation and navigation in space ," *2020 Systems of Signals Generating and Processing in the Field of on Board Communications*, Moscow, Russia, 2020, pp. 1-4, doi: 10.1109/IEEECONF48371.2020. 9078658

8. K. V. Boychenko, I. V. Boychenko, A. Y. Kudryashova, "Interactive Built Space as the New Means of Information Communication," *2019 Systems of Signal Synchronization, Generating and Processing in Telecommunications (SYNCHROINFO)*, Russia, 2019, pp. 1-4, doi: 10.1109/SYNCHROINFO.2019.8813912.

THE INVESTIGATION AND EVALUATION MULTISERVICE NETWORK NGN/IMS FOR MULTIMEDIA TRAFFIC

Bayram G. Ibrahimov
Azerbaijan Technical University, Baku, Azerbaijan, i.bayram@mail.ru

Mehman F. Binnatov
Azerbaijan Technical University, Baku, Azerbaijan

Yalchin S.Isayev
Military Academy of the Republic of Azerbaijan, Baku, Azerbaijan

DOI: 10.36724/2664-066X-2020-6-2-10-13

ABSTRACT

The subject of the study is multiservice communication network using the concept NGN (Next Generation Network) based on the open network architecture IMS (Internet Protocol Multimedia Subsystem), supporting a wide range services. The basis of this architecture is the IMS core, consisting of a set of specialized modules responsible for various functions for customer service. The purpose of the article is to analyze the existing technical capabilities of the IMS multimedia messaging subsystem and perspective solutions for the functioning of the NGN/IMS network efficiency in providing multimedia service. As the efficiency of the system, the capacity NGN/IMS networks is selected using the signaling system and protocols NGN. The capacity NGN/IMS networks during the establishment of a multimedia session was analyzed and the functional architecture of the IMS multimedia messaging subsystem that determine the interaction NGN signaling systems an protocols was explored. Manage the presentation Triple Play services to subscribers and simultaneously modify the media stream within the session allows the protocol for the initialization of the SIP and Diameter sessions, which are the main IMS signaling protocol. One of the important requirements for the IMS subsystem is the maintenance QoS (Quality of Service). A mathematical model for estimating the quality of communication services using a system $GI/G/1/N$ based on the theory diffusion approximation is proposed.

The research presented in this paper is very important for the theory queuing systems, since the article proposes a method for investigating multiservice communication networks with non-Poisson incoming flow and effective results are obtained for NGN/IMS networks. On the basis of the model analytical expressions are obtained, which allow evaluating the performance indicators of the Triple Play service. The proposed mathematical model can be used to solve a wide range of practical problems, including the management multiservice traffic in the process its transmission in multiservice telecommunications networks, taking into account the quality of service classes. Thus, studies NGN/IMS network capacity indicators using SIP protocols are relevant.

KEYWORDS: *throughput, NGN/IMS networks, multimedia session, SIP protocol, IMS subsystem, signaling traffic.*

Information about authors

Bayram G. Ibrahimov, *professor of Azerbaijan Technical University, Baku, Azerbaijan*
Mehman F. Binnatov, *Phd., of Azerbaijan Technical University, Baku, Azerbaijan*
Yalchin S. Isayev, *an associate of the Military Academy of the Republic of Azerbaijan, Baku, Azerbaijan*

Introduction

The constant growth of the volume of transmitted useful and service traffic in multiservice networks with packet switching requires a steady increase in their throughput when establishing a multimedia session, ensuring the quality of service of QoS packets of traffic systems and NGN signaling protocols.

System-technical analysis showed [1-3] that many telecom operators providing multimedia services use service traffic control systems that implement triple play services, such as voice services with the ability to activate multimedia applications, video telephony, IPTV, voice and high-speed access. to the Internet. This approach allows the integration of various services, provides ample opportunities for personalization and increasing the number of multimedia services.

To provide telecommunications operators with the above services in multiservice communication networks, it is necessary to take into account the quality of service QoS of service and useful traffic and perception (Quality of Experience, QoE), which is assessed by several performance criteria [4]. QoS & QoE support is a key requirement for the IMS subsystem and an important indicator of the effectiveness of NGN/IMS networks in establishing a multimedia session. However, this issue has not been studied well enough and remains poorly researched [2-6].

Research problem statement

It is known [3-5] that the connection setup time is the most important QoS indicator of NGN / IMS networks and is determined from the moment when the caller's terminal transmitted all the message necessary to establish the connection until the moment when this terminal equipment (TE) received a signal about the state of the terminal of the called party.

Based on the study, it was determined [2, 4, 6] that the considered NGN/IMS network when servicing traffic packets of systems and signaling protocols is a single-channel queuing system (QS) of the G1/G/1/N type with a limited queue (by designation Kendall-Basharina GI – arbitrary distribution with independent intervals between applications).

Taking into account the nature of the network traffic of NGN/IMS signaling systems and protocols, a mathematical model (MM) of a multimedia service is proposed, taking into account the efficiency indicators of NGN/IMS networks and the features of diffusion approximation methods.

The mathematical formulation of the problem of the proposed MM for assessing the performance indicators of NGN/IMS networks when establishing a multimedia session is described by the following objective function:

$$Q_{эфф.}(\lambda) = W[\arg\max_{i}(C_{i.\max}(\lambda))], \quad i = \overline{1,n}, \qquad (1)$$

under the following restrictions

$$T_{i.cp.з} \le T_{i.cp.з,don.}, \eta_i \ge \eta_{i.don.}, , T_{i.ож.} \le T_{i.ож.don.}, \quad i = \overline{1,n} \qquad (2)$$

where $C_{i.\max}(\lambda)$ – the maximum value of the throughput of NGN / IMS networks with the rate of the incoming stream of service traffic λ when transmitting the *i*-th packet stream; $T_{i.cp.з}$ – average delay time when transmitting the *i*-th packet stream; $T_{i.ож}$ – average waiting time in the queue when servicing the *i*-th packet flow; η_i – efficiency factor of NGN / IMS network resources when transmitting the *i*-th packet stream; $T_{i.cp.з,don.}$ $\eta_{i.don.}$ and $T_{i.ож.don.}$ – accordingly, the admissible values of indicators of NGN / IMS networks when transmitting the i-th packet stream, $i = \overline{1,n}$.

Expressions (1) and (2) define the essence of the considered new approach based on a mathematical model for assessing the quality of communication services.

This paper analyzes a model of the functioning of the efficiency of NGN/IMS networks in the provision of multimedia services, such as voice services with the ability to activate multimedia applications.

The scheme of investigated model functioning of multiservice networks NGN / IMS

Based on the analysis of the quality of work of multiservice communication networks, the functional architecture of IMS was determined, which contains the following levels:

– the level of access and transport;
– sess on management level;
– s rvice and application level.

Figure 1 proposes a diagram of the functioning of the multimedia service traffic model in the NGN/IMS network.

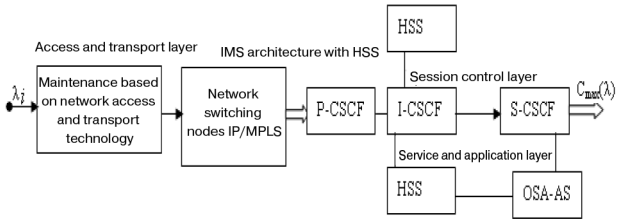

Figure 1. Block diagram of the model functioning servicing traffic in the NGN / IMS network

It follows from the diagram that the algorithm for receiving and serving IMS multimedia traffic begins in the NGN/IMS network at the access network level, as a multi-service access node.

Further, the traffic of the multimedia service is served using the signaling gateway, the core of the IMS network using the HSS-Home Subscriber Server and is transmitted to the AS (Application Server), which interacts with the logical function S-CSGF, I-CSGF and P-CSGF (Serving,

Interrogating, Policy – Call Session Control Function) over SIP.

The analysis shows that the procedure for establishing a multimedia session is initiated by the terminal equipment and the network access gateway, transmitting the INVITE request of the switching nodes using the IP/MPLS protocols through the service access networks and gateways.

Here, SIP is used to establish, control, and disconnect communications. For authorization, authentication and accounting procedures in IMS, the Diameter protocol is also used.

The IMS core using HSS implements request functionality, proxy server functionality, and session management functionality. After receiving and processing, requests and responses of the service by the IMS are sent to the service application server and the service media server.

Evaluation of performance indicators of NGN/IMS networks

From the above described principle of operation of NGN/IMS networks using SIP terminals, it follows that the operation when providing multimedia services and when establishing a session can be considered as a single-phase single-line QS with a finite volume of the buffer storage *N*.

We assume that a stream of traffic packets of signaling protocols with certain characteristics arrives at the input of the buffer storage (BS) of the switching nodes of NGN/IMS networks. Such a model can be analyzed as a general QS *GI*/*G*/1/*N* with a limited queue.

Based on the model, in order to assess the temporal characteristics of NGN/IMS networks when establishing a multimedia session, an approximate analytical method of diffusion approximation can be used, the accuracy of which is within acceptable limits. The idea of the diffusion approximation method is that the distribution Pk of the queue length in the system *GI*/*G*/1/*N* with a limited queue with a total load ρ is approximated by the following distribution [6]:

$$P_k = \begin{cases} 0, & npu \;\; k = 0 \\ (1-\rho\;)(\rho\;)^{k-1}, & npu \;\; k \geq 0 \end{cases} \qquad (3)$$

here P_k – characterizes that at each moment of time k the system has probability distributions of phase states; ρ – load factor of NGN/IMS networks.

In this system, it is assumed that the rate of arrival of service traffic flows λ differs from the Poisson one, and the service process from the exponential distribution law μ. Taking into account the quadratic coefficients of variation of the distribution of intervals C_A^2 between incoming multimedia messages and the distribution of message lengths C_B^2, the load factor of the QS is expressed as follows:

$$\rho \;\; = \exp[(\mu \cdot C_B^2 - \lambda \cdot C_A^2)/2(\lambda - \mu)], \qquad (4)$$

Suppose that due to system failures $\lambda_{обс} = 0$.

Then, the mean $E[T_{отк}]$ the failure time interval is expressed as follows:

$$E[T_{отк}] = \frac{\lambda_{вх} \cdot \lambda_{вых}}{\lambda_{вх} - \lambda_{вых}} \leq T_{отк.доп}, \qquad (5)$$

where $\lambda_{вх}$, $\lambda_{вых}$ – accordingly, the rate of the incoming and outgoing packet traffic of the NGN/IMS protocols when establishing multimedia sessions.

Thus, based on the model $GI/G/1/N_{бн}$ of expression (5), the average failure time is characterized and is an indicator of QoS & QoE.

Determining the capacity of NGN/IMS networks when establishing a multimedia session

Taking into account the features of the general QS type *GI*/*G*/1/*N* with a limited queue, the average queue length $E[L_{ср}]$ in BS switching nodes of NGN/IMS networks can be determined by Little's formula by the following expression:

$$E[L_{ср}] = \lambda_{вх} \cdot \{1 - E[P_{отк}]\} \cdot E[T_{ож}], \qquad (6)$$

Based on the proposed MM, the average time to establish a multimedia session for providing Triple Play services, corresponding to the average stay time of traffic packets in the NGN/IMS switching node, is expressed as follows:

$$E[T_{уст.}] = \{E[T_{ож}] + \mu^{-1}\} \cdot (1 - P_{отк}), \qquad (7)$$

It should be noted that expressions (6) and (7) determine the probabilistic-temporal characteristics of systems and signaling protocols of NGN/IMS networks and are indicators of the quality of service QoS of multiservice traffic.

Taking into account (5), (6) and (7) the maximum value of the throughput of NGN/IMS networks when establishing a multimedia session is determined as follows:

$$C_{\max}(\lambda) = 1/E[T_{уст}(\lambda)], \qquad (8)$$

The last obtained expressions (5), (6), (7) and (8) are an indicator of the effectiveness of NGN/IMS networks in establishing a multimedia session.

Numerical analysis results

Figure 2 shows the dependence of the NGN/IMS network bandwidth on the system load factor and the transmission rate of multimedia traffic.

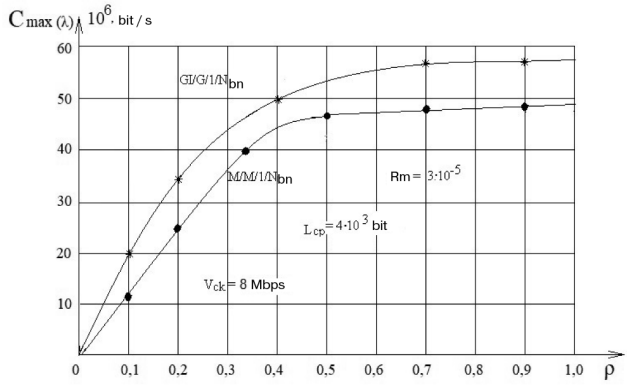

Figure 2. Graphical dependence of NGN/IMS network bandwidth on the system load factor when establishing a multimedia session

Graphical ndency family analysis $C_{\max}(\lambda) = W(\rho, \lambda_{вх}, V_{ck})$ shows that with an increase in the CMO load factor, the NGN/IMS throughput using the HSS home subscriber servers increases, thereby reducing the average multimedia session setup time for a given $V_{ck} = 155$ Mbit/s.

Thus, a comparative analysis of the QS of the general type *GI*/*G*/1/*N* and *M*/*M*/1/*N* shows that the contribution of the IMS core to the delays in establishing a multimedia session is significant and should be taken into account when designing NGN/IMS networks.

Conclusions

As a result of the study, an MM was proposed, in the form of a QS of the general type *GI*/*G*/1/*N* with queues, based on the approximate method of diffusion approximation. Analytical expressions have been obtained that make it possible to assess the quality of service QoS & QoE of multiservice traffic and analyze the characteristics of the NGN/IMS network bandwidth when establishing a multimedia session.

References

1. E. E. Malikova, A. P. Pshenichnikov. “Calculation of the volume equipment for multiservice communication networks,” Moscow: Hot line-Telecom. 2017. 90 p.

2. B. Ya. Likhtzinger. “Interval method of queuing analysis in queuing systems with packets requests,” *T-Comm*. 2017. Vol. 11. No3. P. 1 3.

3. K. Ye. Samuylov, M. V. Luzgachev, O. N. Plaksina. “Development of a probabilistic model for analyzing the quality indicators of the protocol for initiating communication sessions,” *Vestnik of the PFUR. Series Mathematics. Computer science. Physics*. 2007. No. 3-4. P. 16-26.

4. B. G. Ibragimov, S. R. Ismailova. “Investigation and analysis of the effectiveness multiservice communication networks using the architectural concept NGN,” *T-Comm*. 2014. Vol. 8, No 8. P. 47-50.

5. J. G. Van Bosse, F. U. Devetak. Signaling in Telecommunications Networks. NY: John Wiley, 2007. 810 p.

6. A. R. Ward, P. W. Glinn. “A diffusion approximation for a GI/G/1 queue with balking or reneging,” *Queueing Systems*. 2005. Vol. 50. No. 4. P. 371-400.

QUALITY OF SERVICE ASSESSMENT IN LTE NETWORKS WITH A LIMITED NUMBER OF USERS

Ndayikunda Juven,
University of Bujumbura, Bujumbura, Burundi,
juvndayi@mail.ru

DOI: 10.36724/2664-066X-2020-6-2-14-19

ABSTRACT

Narrow Band Internet of Things (NB-IoT) is the latest cellular radio access technology that was based on LTE technology and implemented as part of the 3GPP 3GPP 3GPP for Low-power Wide-area Network (LPWAN). The paper considers the features of NB-IoT standards based on the characteristics of the physical and channel layers of NB-IoT technology based on release 14-15 of the 3GPP group. The aim of this work is also to build and study a model for serving heterogeneous traffic in an isolated cell of the LTE standard, which supports the functionality of the Internet of Things IoT (Internet of Things), in particular eMTC (enhanced Machine Type Communication). The constructed mathematical model takes into account the heterogeneity of the arrival of requests and their dependence on the number of users of cellular services. Depending on the number of sources, incoming requests are described by Poisson or Engset models. The studied model makes it possible to dynamically allocate resources that have LTE.

KEYWORDS: *Internet of Things (IoT), LTE, eMTM, dynamic allocation, rate of lost requests, resource blocks, NB-IoT, bandwidth*

INTRODUCTION

The current stage of development of infocommunication networks requires solving urgent problems of analyzing the characteristics of the quality of service of incoming requests. Over the past few years, there has been a rapid growth in the number of telecommunication devices. According to Cisco forecasts, the number of devices connected to the Internet is growing rapidly and already exceeds the world's population [1, 2]. These include eMTC devices and various IoT sensors [6]. The increase in the number of devices connected to the Internet has made it necessary to develop new methods for assessing the quality of communication. The existing communication infrastructure is used to transfer the data traffic. Such networks are often deployed in locations where wired communication is limited. Wired Internet connection of telecommunication devices is not always possible in some areas. For the transmission of video information, voice messages, etc. in such places where there is no possibility of using wired communication at all, a wireless communication network is used. The LTE standard in the last 10 years has been a leader in the field of mobile communications.

In 2014, the 3rd Generation Partnership Project (3GPP) began development on the Internet of Things standard i.e. provision of services to users using the technology "energy efficient long-range network LPWAN (Low-power Wide-area Network)". In the LPWAN category, there are licensed technologies such as M1 (LTE-M) and unlicensed technologies, for example. Long Range (LoRa), SigFox, Ingenu, etc. In this paper, we consider servicing requests from a finite number of users, which are surveillance cameras and requests from traditional LTE devices.

This paper examines the features of the NB-IoT standard in comparison with the characteristics of LTE technology at the physical layer. When writing this article, the materials of the LTE Rel.14, 15 specifications were used, published in December 2016 - November 2017.

Formulation of the problem

Let's consider a cellular communication of the LTE standard providing information transfer to the analytical center. The available radio resources of an LTE cell in the uplink direction are measured in terms of their smallest granularity, called a channel or unit resource. The total number of unit resources is a linear function of the number of RB (Resource Blocks).

In the investigated cell of the LTE standard, there are a number of LTE devices and IoT devices connected to the base station. LTE devices and IoT devices are sources of requests [7]. For simplicity of calculations, it is assumed that its base station is located in the center of the cell, all claims equally use the base station resource allocated to one claim, regardless of the distance between the base station and the terminal. The selection of active devices is performed in a circular cyclic scheme (Round Robin) as shown in [3].

Let s be the number of video surveillance devices with high quality of service. To transmit video information of such devices, it is necessary to use a large number of channel units.

Table 1

Number of resource blocks depending on the channel width

Channel width, MHz	1,4	3	5	10	1	
Number of resource blocks	6	15	25	50		

Let me denote by v – the total number of units of the required channel resources (the total number of channel units). Let us recall that in the fourth generation mobile communication network built according to the LTE standard, the resource is resource blocks that depend on the frequency band (Table 1).

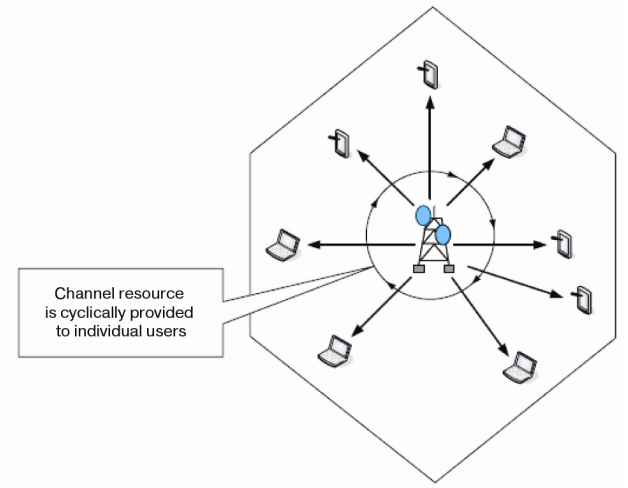

Figure 1. Scheme of active subscribers cyclic service in a cell

Denote by β exponential distribution parameter of time interval before sending the corresponding request from one source from final group of users.

Intensity of IoT requests receipt depends on the number of active video surveillance devices and is equal to $(s-i_1)\beta$, where i_1 is the number of requests from origin in target group of users in service.

Denote by b_1 – the number of channel units needed to service one request created by a limited number of video surveillance devices. The intensity of the proposed traffic is determined by the following formula [4]:

$$a_1 = \frac{s\beta}{\mu_1 + \beta};$$

where μ_1 is a parameter of exponential distribution of service time interval for requests from a finite user group source.

The constructed model takes into account the heterogeneity of incoming traffic flows, i.e. dependence of receipt intensity and requests processing on the traffic type. Model receives the second type of requests originating from a large number of LTE devices. Based on this assumption, a change in their numbers does not greatly affect intensity of incoming requests. In this case, we can use the Poisson model to describe the process of incoming requests.

The arrival of requests from traditional LTE devices obeys Poisson's law with an intensity λ. To service the incoming request, b_2 channel units are used. The suggested traffic intensity is determined using the following expression:

$$a_2 = \frac{\lambda}{\mu_2},$$

where μ_2 – parameter of request servicing time intervalexponential distribution.

Markov process and quality of service characteristics

Let $i_1(t)$ be the number of requests for the transmission of video information in service at a point in time $t \geq 0$ and $t \geq 0$ - the number of requests from traditional LTE devices in service at a point in time $t \geq 0$. The change in the state of the model is described by a random Markov process $r(t) = (i_1(t), i_2(t))$ defined on the state space *S*, consisting of vectors (i_1, i_2) with components:

$$i_1 = 0,1,\ldots,\min\left(s_1, \left\lfloor \frac{v}{b_1} \right\rfloor\right);$$

$$i_2 = 0,1,\ldots,\left\lfloor \frac{v - i_1 b_1}{b_2} \right\rfloor.$$

Let us denote i by the number of cell resource units occupied in the state of servicing video traffic (i_1, i_2) and traffic from traditional LTE devices and is defined as the total product of the number of requests being serviced at a point in time $t \geq 0$ and the number of channel units required to transmit the corresponding requests ($p(i_1, i_2)$ – stationary probability of the model (i_1, i_2) state).

It is convenient to compose the equations of statistical equilibrium of the system following the following rule: the total incoming flow of probabilities into the state (i_1, i_2) must be equal to the total outgoing flow of probabilities from the state of the carrot process (i_1, i_2) model $r(t)$ in its stationary mode. Using the indicator of the function, we represent all the equations of the system of equations of equilibrium of states in one relation, which makes it convenient for the implementation of iterative algorithms for solving the corresponding system.

The system of equilibrium equations connecting the unnormalized probabilities has the form:

$$\begin{aligned} & P(i_1, i_2)\{(s - i_1)\beta I(i + b_1 \leq v) + i_1\mu_1 I(i_1 > 0) + \\ & \quad + \lambda I(i + b_2 \leq v) + i_2\mu_2 I(i_2 > 0)\} = \\ & = P(i_1 - 1, i_2)(s - i_1 + 1)\beta I(i_1 > 0) + \\ & \quad + P(i_1, i_2 - 1)\lambda I(i_2 > 0) + \\ & + P(i_1 + 1, i_2)(i_1 + 1)\mu_1 I(i + b_1 \leq v, i_1 + 1 \leq s) + \\ & + P(i_1, i_2 + 1)(i_2 + 1)\mu_2 I(i + b_2 \leq v). \end{aligned} \quad (1)$$

Let us denote by π_1 and π_2 the shares of the time of resource occupancy at the moment of receipt of an application for servicing video traffic and traffic from traditional LTE devices, respectively. Let us denote by $\pi_{1,c}$ and $\pi_{2,c}$ the shares of lost requests for the transmission of video traffic and traffic from endless traditional LTE devices, respectively.

Let us denote by m_1 and m_2 - the average number of resource units occupied in the state of (i_1, i_2) servicing video traffic and traffic from traditional LTE devices, respectively.

The average number of requests for video traffic and traffic transmission from traditional LTE devices will be denoted by y_1 and y_2 respectively.

$$\pi_k = \sum_{(i_1, i_2) \in S \mid i + b_k > v} p(i_1, i_2); \quad k = 1, 2;$$

$$\pi_{1,c} = \frac{\sum_{(i_1, i_2) \in S \mid i + b_1 > v} p(i_1, i_2)(s - i_2)\beta}{\sum_{\{(i_1, i_2) \in S\}} p(i_1, i_2)(s - i_2)\beta};$$

$$\pi_{2,c} = \pi_2 \ ;$$

$$m_k = \sum_{(i_1, i_2) \in S} p(i_1, i_2) i_k b_k; \quad k = 1, 2;$$

$$y_k = \sum_{(i_1, i_2) \in S} p(i_1, i_2) i_k; \quad k = 1, 2.$$

To assess the listed service quality indicators, it is necessary to find the value $p(i_1, i_2)$ by solving the equilibrium equation system (1) by the iterative Gauss-Seidel method [5].

LTE base station resource with NB-IoT functionality. LTE frame structure

In the past 10 years, there has been a rapid growth in the number of wireless communications. According to Cisco's forecast, the number of devices connected to the Internet is growing rapidly (10% CAGR (Compound annual growth rate)) and already exceeds the world's population [2-3]. A significant proportion of such devices are focused on transmitting a small amount of information (NB-IoT files) at a rate of ~ 250 kbit/s and ~ 226.7 kbit/s via the downlink and uplink, respectively.

There is a need to connect a huge number of devices to the Internet. Therefore, the 3GPP consortium has implemented the NB-IoT narrowband Internet of Things standard as a solution to this problem. NB-IoT is classified as one of the licensed low power, long range, and low cost cellular technologies for wide area LPWANs based on LTE technology. There are other licensed technologies in the LPWAN category, such as M1 (LTE-M), and unlicensed technologies, for example. Long Range (LoRa), SigFox, Ingenu, etc.

The radio interface of the LTE technology is based on the Orthogonal Frequency-Division Multiplexing OFDM technology. In order to increase the data transfer rate, LTE networks use the technology of multi-antenna systems MIMO (Multiple Input Multiple Output).

OFDM technology assumes the transmission of a wideband signal through the independent modulation of narrowband subcarriers of the form $s_k = a_k \sin[2\pi(f_0 + k\Delta f)]$ that are located with a certain frequency step Δf . The OFDM symbol contains a set of modulated subcarriers, a payload field and a so-called Cyclic Prefix CP. In LTE standard, the step between subcarriers Δf is 15 kHz, which corresponds to an OFDM symbol duration of 66.7 μs.

Each subscriber unit in a slot is assigned a specific range of channel resources in the frequency time domain (Figure 2). The length of an LTE frame is 10ms and each frame is divided into 10 subframes of 1ms each. One subframe contains two slots. The duration of each slot is 0.5ms. Depending on the cyclic prefix configuration, each slot has 7 and 6 OFDM symbols.

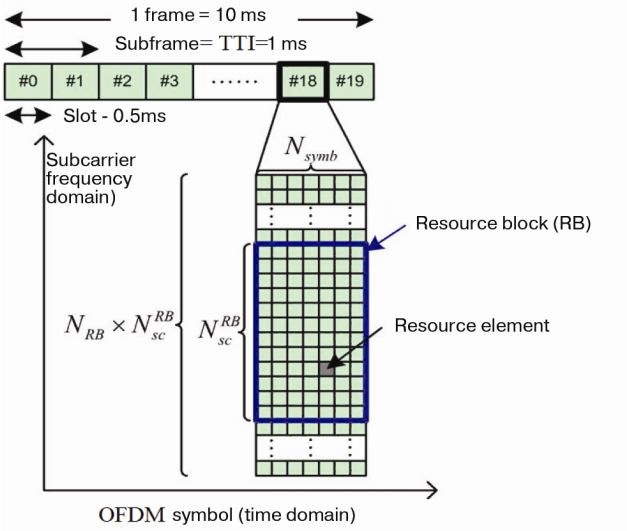

Figure 2. LTE frame structure

In the frequency domain, each channel resource consists of Resource Blocks. In turn, each resource block consists of 12 adjacent subcarriers, occupying a bandwidth of 180 kHz (Fig. 1). The number of resource blocks depends on the channel bandwidth and varies from 6 to 110 resource blocks [2].

The resource block is the main resource unit for scheduling data transmission in the radio interface and is the minimum resource element allocated to the subscriber unit by the base station scheduler.

Features of the technology of narrowband Internet of things NB-IoT

NB-IoT devices can operate at lower signal levels, hence higher noise levels. Another advantage is the battery saving [5]. NB-IoT technology is designed for short message transmission only, not for transmission of audio / video content or large files.

This section discusses the features of the physical layer of NB-IoT technology. Also presented is a stack of NB-IoT protocols, based on modern PHY and MAC levels, in order to identify the knowledge gap and determine the direction of development of narrowband Internet of things technology.

Infrastructure of NB-IoT standard network is deployed on top of the existing LTE infrastructure. The 3GPP consortium offers three options for deploying NB-IoT networks: narrow-band Internet of things on the guard band (NB-IoT Guard Band), in-band (In Band), and stand-alone (Stand Alone) (Fig. 3).

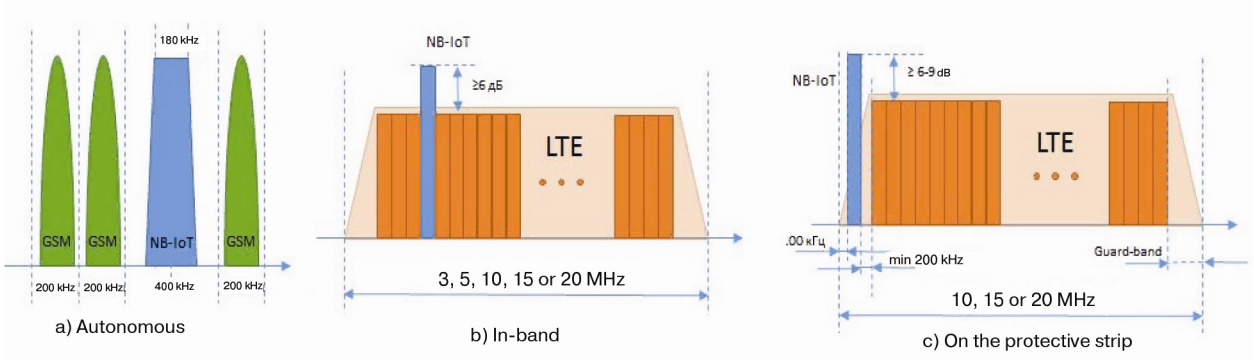

Figure 3. Deployment options for narrowband Internet of things

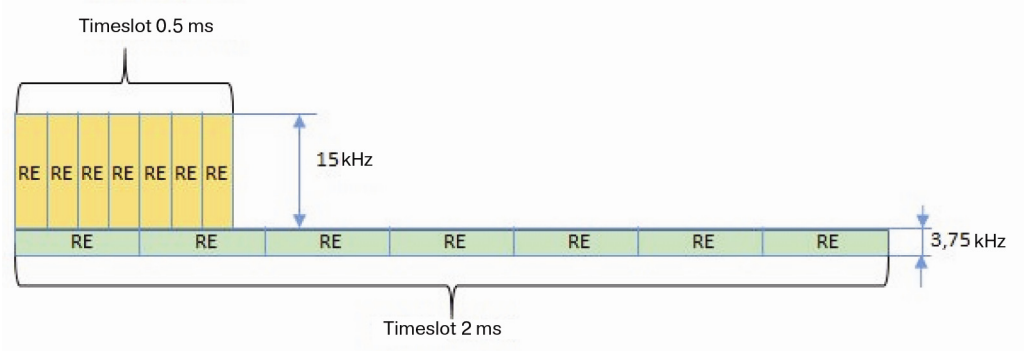

Figure 4. Resource element

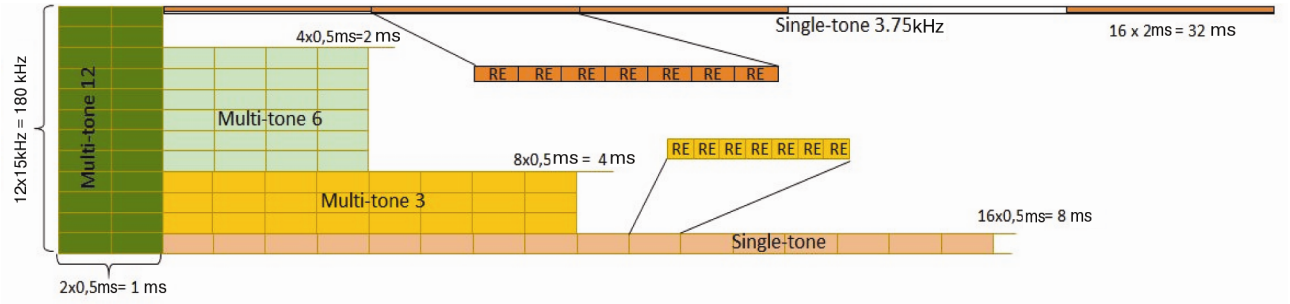

Figure 5. Single resource RU [9]

Physical channels and signals

NB-IoT standard adopts the same frame structure as LTE [6-8]. One superframe consists of 1024 frames, which in turn contain 10 subframes each. One subframe contains two time slots of 0.5 ms each in the time domain. In the frequency domain, either 12 subcarriers are used in each 0.5 ms slot, or 48 subcarriers are used with a 2 ms slot at a spacing frequency of 3.75 kHz in the uplink.

NB-IoT uses the same protocol stack as LTE. However, some design changes at both the PHY and MAC levels have been introduced to support massive long distance connections with MCL (Maximun Coupling Loss) up to 20 dB compared to traditional technologies such as LTE, GSM and GPRS [1].

At the physical layer of NB-IoT, the same technologies are used as in LTE. OFDM and SC-FDMA technologies are used in the NB-IoT standard to generate signals on the transmission of information in the downlink and uplink, respectively. However, the resource scheduling block in NB-IoT is a resource element RE (Resource Element) (or tone) instead of PRB (Physical Resource Block), allowing NB-IoT devices to transmit a signal on a single subcarrier at 15 kHz, which makes it possible to serve multiple users in a frequency band 180 kHz.

Signal transmission in a narrow band on a single subcarrier of 15 kHz, and the same at a lower frequency of 3.75 kHz, can significantly increase the spectral density of the signal and, therefore, the signal-to-noise ratio increases, which is very important for subscriber devices that have much less powerful transmitters than the base station.

Support for multi-tone transmission – Multi-Tone Transmission

To connect mass devices to one base station, NB-IoT distributes resource units (RU — Resource Units) among several user devices, in contrast to LTE, where the entire resource unit is allocated to one user in the uplink [1].

The uplink communication uses the SC-FDMA multiplexing scheme. The frequency spacing between subcarriers is 3.75 kHz or 15 kHz. On the downlink, NB-IoT uses 15 kHz with OFDM, just like LTE. With 15 kHz spacing, NB-IoT can allocate both single-tone (8ms) and multi-tone (3 tones, 6 tones, and 12 tones) to different users in 4ms, 2ms and 1ms durations, respectively. With 3.75 kHz, only single-tone is supported with 48 subframes of 32 ms duration. RU is another larger brick from which transport blocks (Transport blocks, TB), assigned to the user, are formed.

Conclusion

This article discusses dynamic resource allocation for sharing real-time IoT traffic streams, packet data, and traffic from traditional LTE devices over radio resources of an LTE cell. In the constructed model, two types of flows were considered. The first type of traffic represents streams coming from sources from the end user group and the second from traditional LTE devices. Depending on the number of sources, incoming requests are described by Poisson or Engset models.

All the random parameters used in the model have an exponential distribution with corresponding mean values. And also in the work, a model for assessing the quality of service requests in a mobile communication network of the LTE standard is built, taking into account the heterogeneity of incoming traffic flows.

The analysis process of applications joint service in isolated cell of the LTE standard, which supports the IoT functionality, in particular, eMTM, is carried out. Using the constructed model, the main indicators of the quality of service are determined on the basis of obtained values of the limiting probabilities of model stationary states.

Investigated model allows to dynamically distribute the available resource between incoming requests. The constructed model provides operators with additional opportunities to improve quality of LTE cellular network.

The LTE base station with NB-IoT functionality uses DCI (Downlink Control Information) to transmit downlink / uplink scheduling overhead to NB-IoT. Then, based on the scheduling information received, the NB-IoT user equipment (UE) determines the deployment mode of the NB-IoT network (autonomous mode, in-band mode or in the guard interval), as well as cell identification and

finds out which resource elements are already in use in LTE.

Thus, the UE can map the PDCCH and PDSCH symbols into available resource elements. For example, in the downlink, NPDCCH is transmitted by aggregating narrowband control elements (entry 0 and entry 1), where entry 0 is transmitted by subcarriers 0 through 5 and entry 1 using subcarriers 6 through 11 in a subframe.

In addition, DCI can be multiplexed in one subframe, or one DCI can be mapped in one subframe, according to the aggregation level used. NB-IoT uses limited BPSK and QPSK modulation schemes with support for only one antenna, both in uplink and downlink.

References

1. Collins Burton Mwakwata, Hassan Malik, Muhammad Mahtab Alam, Yannick Le Moullec, Sven Parand, Shahid Mumtaz. Narrowband Internet of Things (NB-IoT): From Physical (PHY) and Media Access Control (MAC) Layers Perspectives. *Sensors (Basel)*. 2019 Jun 8.
2. 3GPP ETSI TS 136 300 V14.3.0. LTE; Evolved Universal Terrestrial Radio Access (E-UTRA) and Evolved Universal Terrestrial Radio Access Network (E-UTRAN); Overall description. 2017. 347 p.
3. 3GPP TS 36.101 V15.0. Evolved Universal Terrestrial Radio Access (E–UTRA). User Equipment (UE) radio transmission and reception. 2017. 1547 p.
4. Ryzhkov A.E. Development of NB-IoT technology. *Proceedings of educational institutions of communication*. 2017. Vol. 3. No. 4. P. 94-101.
5. Salman, L., Salman, S., Jahangirian, S., Abraham, M.; German, F., Blair C., Krenz P. Energy efficient IoT-based smart home. *IEEE 3rd World Forum on Internet of Things (WF-IoT),* Reston, VA, USA, 12-14 December 2016.
6. Beyene Y.D., Jantti R., Tirkkonen O., Ruttik K., Iraji S., Larmo A.; Tirronen T.; Torsner J. NB-IoT Technology Overview and Experience from Cloud-RAN Implementation. *IEEE Wirel. Commun*. 2017, 24, pp. 26-32.
7. Xu T.; Darwazeh I. Non-Orthogonal Narrowband Internet of Things: A Design for Saving Bandwidth and Doubling the Number of Connected Devices. *IEEE Internet Things J.* 2018, 5, 2120-2129.
8. Adhikary A., Lin X., Wang Y.E. Performance Evaluation of NB-IoT Coverage. *IEEE 84th Vehicular Technology Conference (VTC-Fall),* Montreal, QC, Canada, 18-21 September 2016.
9. Ilnur Fauziev. NB-IoT: how does it work? Part 1. URL: https://habr.com/ru/company/ru_mts/blog/430496/ (date of access 10.12.2019).
10. Cisco Visual Networking Index: Forecast and Methodology, 2017–2022, February, 2019.
11. Stepanov S.N. Teletraffic theory: concepts, models, applications. Series "Theory and Practice of Infocommunications". Moscow: Hotline - Telecom, 2015. 868 p.
12. Huawei Global Industry Vision 2025, 2018.
13. Stepanov S.N., Romanov A.M., Osiya D.L. Construction and analysis of a data transmission model on an access line from a finite group of subscribers. *T-Comm*. 2015. Vol. 9. No. 9. P. 29-34.
14. Stepanov S.N., Stepanov M.S., Malikova E.E.,
15. Tsogbadrakh A., Ndayikunda J. Construction and analysis of a generalized resource sharing model for LTE technologies with NB-IoT functionality. *T-Comm*. 2018. Vol. 12. No. 12. P. 71-77.
16. Victor Alekseev. Quectel modules with NB-IoT and eMTC support. *Wireless technology*. No.2. 2018. P. 9-16.
17. Begishev V., Petrov V., Samuylov A., Moltchanov D., Andreev S., Koucheryavy Y., Samouylov K. Resource Allocation and Sharing for Heterogeneous Data Collection over Conventional 3GPP LTE and Emerging NB-IoT Technologies. *Computer Communications*. 2018. Vol. 120. No. 2. P. 93-101.

DYNAMIC PARAMETERS OF ELASTIC PLATE OPTICAL SWITCH DRIVES

Vagif Ali Magerramov,
Baku Technical University, Baku, Azerbaijan, mvg476@mail.ru

Mehman Huseyn Hasanov,
Baku Technical University, Baku, Azerbaijan, mhasanovnew@gmail.com

DOI: 10.36724/2664-066X-2020-6-2-20-23

ABSTRACT

The methods and means of improving the efficiency and the parameters of the dynamic parameters of the elastic plate of the optical commutator drive using advanced information and telecommunication technologies are analyzed. The bandwidth of optical communication networks based on systems with flat spring-loaded optical drive switch rods is investigated. On the basis of the study, the dynamic parameters of the elastic plate of the optical commutator drive are proposed a structural-functional scheme of a system with flat spring-loaded plates and linear algebraic equations for the dynamics of an elastic plate with the aid of which the equation for small oscillations of a rod near a rectilinear position is compiled. The equations of dynamics of systems with flat spring-loaded optical drive switch rods are considered and determined. On the basis of the system-technical analysis, a general integral of the spring deflection equation is determined. With the help of the solution, the equation for the dynamics of an elastic plate obtained a mathematical expression of the displacement of the upper end of the rod vertically of the spring-loaded drive system of the optical commutator.

KEYWORDS: *dynamics equations, optical commutator drive, integral of the deflection equation, fiber-optic networks*

Information about authors

Vagif Ali Magerramov, *Doctor of Mathematics, Professor, The department "Radiotexnika and televisons systems", Baku Technical University, Baku, Azerbaijan*

Mehman Huseyn Hasanov, *Cand. Tech Science, Associate Professor, The Department "Multi-channel telecommunication systems", Baku Technical University, Baku, Azerbaijan*

Introduction

The main advantage of fiber-optic networks is their practically unlimited bandwidth. The practical value of this property lies in the possibility of a multiple increase in the speed of information transmission over fiber-optic communication channels on a global scale. This makes research in the field of optical networks very relevant and promising.

Systems with flat spring-loaded (Fig. 1) plates and other microelectromechanical and piezoceramic drives [1, 2] can be used as a drive in the switch.

As noted in [1], each linear-translational motion drives under the action of signals from the switch control unit can be in a passive (recessed) or active (vertical) position.

As can be seen from Figure 1, a semitransparent mirror in the passive position can pass the optical beam (Fig. 1a), or deflect the beam at an angle of 90o, dividing it into two equal flows (Fig. 1b).

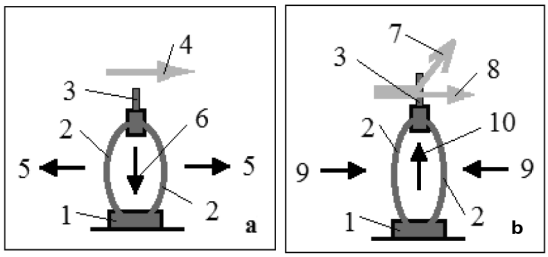

Figure 1. Kinematics of a system with flat spring loaded plates:
1 – base; 2 – spring-loaded plates; 3 – translucent mirror; 4 – optical beam of direct passage; 5 – pulling force of the plates; 6 – direction of decreasing the height of the system (drowning the translucent mirror) downward; 7 – deflected beam; 8 – beam passed through a semitransparent mirror; 9 – force of compression of plates; 10 – directions of increasing the height of the system (falling of the translucent mirror) up.

A distinctive feature of the system with flat spring-loaded plates (Fig. 1) is that due to the spring-loaded drive [3], when the acting voltage is removed, the system returns to its original (initial) position. In the system, both electromagnetic and piezoelectric translational drive can be used as a drive.

1. uation of dynamics of an elastic plate

Consider a system with flat spring-loaded plates [3], in which there are two elastic plates A and B with a given length *L* and rigidity *C*. On them, as shown in Fig. 1a, a semitransparent mirror of mass *m* is attached. To obtain the dynamic equation of this system $\pm F(t)$, we divide the spring-loaded plates into two parts along the line as shown in Fig. 1b. We will assume that acting on one of the plates with a force, we thereby force it to contract or lengthen (respectively, the other plate will contract or lengthen), and the height of the plate (in Fig.1b) is shortened or lengthened by $\pm \Delta x$. The force exerts a similar effect $\pm F(t)$ on the other plate.

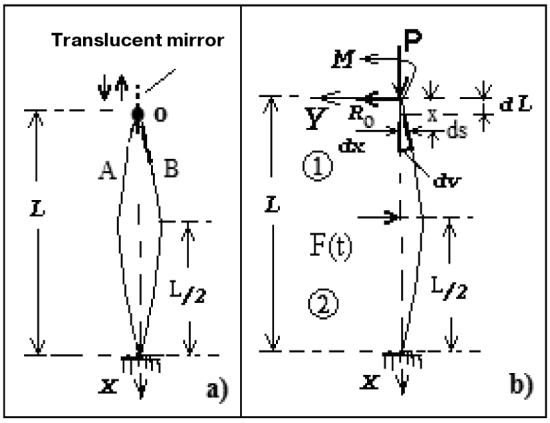

Figure 2. Kinematics of an elastic plate

In the given problem, the elastic rods under the action of the force $\pm F(t)$, the gravity force *m* of the mirror and the rigid support, as well as the conditions of attachment at the ends, will be in conditions of longitudinal-transverse bending (Fig. 2b). Since the end of the rod is considered rigidly fixed, then when the rod is curved, in addition to the reaction force R_0, there is also an end moment M_0. The force P is equal to half the weight of the mirror and the rigid support $P = mg/2$. The second part of the weight of the mirror and rigid support comes from the other rod.

Compose the equation of small vibrations of the rod near the rectilinear position. We assume that the distributed mass of the rod is negligible in comparison with the mass of the mirror and the rigid support, while neglecting the resistance forces, the equation of small vibrations has the form [4]:

$$EI\frac{\partial^2 \vartheta}{\partial x^2} = -p\vartheta + M \tag{1}$$

where $v(x,t)$ – dynamic deflection at each point, E – modulus of elasticity, I – moment of inertia, $M(x,t)$ – dynamic bending moment arising in the cross-sections of the bar as a result of transverse load and support reactions.

We divide the rod into two (1 and 2) sections, then the bending moment will be:

in the first section $M_1 = R_0(t) - M_0(t)$ (2)

in the second section $M_2 = R_0(t)x - M_0(t) + F_2(t)\left(x - \frac{L}{2}\right)$ (3)

Then, in the first section, we get the following differential equation:

$$\frac{\partial^2 \vartheta_1}{\partial x^2} + K_0^2 \vartheta_1 = \frac{1}{EI}\left[-R_0 X - M_0\right] \tag{4}$$

in the second section:

$$\frac{\partial^2 \vartheta_2}{\partial x^2} + K_0^2 \vartheta_2 = \frac{1}{EI}\left[- R_0 X - M_0 + F\left(X - \frac{L}{2}\right)\right] \tag{5}$$

where the notation is introduced: $K_0^2 = P/EI$; $P = mg/2$.

It is known that [5], the equations of small oscillations can be satisfied with the expressions:

$$\begin{aligned} \vartheta(x,t) &= V(x)e^{i\cdot\omega\cdot t} \\ F_2(t) &= Fe^{i\cdot\omega\cdot t} \\ R_0(t) &= R_0 e^{i\cdot\omega\cdot t} \\ M_0(t) &= M_0 e^{i\cdot\omega\cdot t} \end{aligned} \tag{6}$$

here ω is some constant.

Substituting expressions (6) into (4) and (5), get:
in the first section:

$$\frac{d^2 V_1}{dx^2} + K_0^2 V_1 = \frac{1}{EI}\left(- R_0 X - M_0\right) \tag{7}$$

in the second section:

$$\frac{d^2 V_2}{dx^2} + K_0^2 V_2 = \frac{1}{EI}\left[- R_0 X - M_0 + F\left(X - \frac{L}{2}\right)\right] \tag{8}$$

Then, the general integral of equations (7) and (8), respectively, will be:

$$V_1(x) = C_1 SinK_0 X + C_2 CosK_0 X - \frac{1}{EIK_0^2}\left(R_0 X + M_0\right) \tag{9}$$

$$V_2(x) = C_3 SinK_0 X + C_4 CosK_0 X - \frac{1}{EIK_0^2}\left[R_0 X + M_0 - F\left(X - \frac{L}{2}\right)\right] \tag{10}$$

As can be seen from (9) and (10), in each section the deflection linearly depends on the constant parameters in the first and second sections: C_1, C_2, C_3, C_4, R_0 and M_0.

These constant coefficients are determined from the conditions for fixing the plate at the ends and the conditions of continuity during the transition from the first section to the second.

In the case considered in Fig. 2b case, these conditions are as follows:

$$\begin{array}{lccc} \text{at} & x = 0 & V_1(0) = 0 & V_1^I(0) = 0 \\ \text{at} & x = L/2 & V_1(L/2) = V_2(L/2) & V_1^I(L/2) = V_2^I(L/2) \\ \text{at} & x = L & V_2(L) = 0 & V_2^I(L) = 00 \end{array} \tag{11}$$

Using boundary conditions (11) from (9) and (10) after some transformations [4], we obtain a system of six linear algebraic equations, from the solution of which we finally obtain the desired constant coefficients:

$$\begin{aligned} C_1 &= \frac{F}{2K_0 P}; \\ C_2 &= -\frac{F}{2K_0 P}\frac{Sin(\alpha/2)}{Cos(\alpha/2)}; \\ C_3 &= -\frac{F}{2K_0 P}\frac{Cos(3\alpha/2)}{Cos(\alpha/2)}; \\ C_4 &= \frac{F}{2K_0 P}\frac{Sin(3\alpha/2)}{Cos(\alpha/2)}; \\ R_0 &= \frac{F}{2}; \\ M_0 &= -\frac{F}{2K_0}\frac{Sin(\alpha/2)}{Cos(\alpha/2)} \end{aligned} \tag{12}$$

where $\alpha = L\cdot\sqrt{\frac{3\cdot m\cdot g}{2\cdot b\cdot h^3\cdot E}}$ – constant parameter, b – width and h – plate thickness.

Then the general integral of the deflection equation, in the first and second sections, respectively, will be:

$$V_1(x) = C_1\left(SinK_0 X - K_0 X\right) + C_2\left(CosK_0 X - 1\right) \tag{13}$$

$$V_2(x) = C_3 SinK_0 X + C_4 CosK_0 X - C_1 K_0 X - C_2 + \frac{F}{P}\left(X - \frac{L}{2}\right) \tag{14}$$

Taking into account (12) in (13), finally, in the first section get:

$$V_1(x) = \frac{F\cdot L}{4P}\cdot A_1(x) \tag{15}$$

where

$$A_1(x) = \frac{1}{\alpha}\left[SinK_0 X + tg\frac{\alpha}{2}\left(1 - \cos K_0 X\right) - K_0 X\right]$$

Taking into account (12) in (14), finally, in the second section get:

$$V_2(x) = \frac{F\cdot L}{4P} A_2(x) \tag{16}$$

where

$$A_2(x) = \frac{1}{\alpha}\left[\frac{Sin\left(\frac{3\alpha}{2} - K_0 X\right)}{Cos\frac{\alpha}{2}} + K_0 X - 2\alpha + tg\frac{\alpha}{2}\right]$$

2. V tical offset of the upper end of the bar

One of the important parameters of the optical commutator drive with the proposed flat spring-loaded rods is the displacement of the upper end of the rod on which the semitransparent mirror is fixed (position 3 in Fig. 1). Therefore, after determining the deflection, we determine the vertical displacement of the upper end of the bar.

With lateral deflection, the centerline of the bar is initially compressed, and the upper part of the spring-loaded system is somewhat lengthened. We assume that the rod is not extensible. Therefore, consider an element dS of the curved axis of the beam (Fig. 2b). Let dX is its projection onto the axis X, then there will be a bend dV. The vertical offset of the top end of the bar will be:

$$\Delta L = \int_0^L dL = \int_0^L (dS - dX) = \int_0^L \left[\left(\sqrt{1 + \left(\frac{dV}{dX} \right)^2} \right) dX - dX \right] \approx \frac{1}{2} \int_0^L \left(\frac{dV}{dX} \right)^2 dX; \tag{17}$$

To determine the vertical displacement of the upper end of the bar ΔL, we use solutions (9) and (10). Then the total rod elongation has:

$$\Delta_L = \Delta_{L1} + \Delta_{L2} \tag{18}$$

where

$$\Delta L_1 = \frac{1}{2} \int_0^{L/2} \left(\frac{dV_1}{dX} \right)^2 dX \tag{19}$$

$$\Delta L_2 = \frac{1}{2} \int_{L/2}^{L} \left(\frac{dV_2}{dX} \right)^2 dX \tag{20}$$

Taking into account (15) in (19) and (16) in (20) and after transformation, we finally obtain the mathematical expression for the vertical displacement of the upper end of the rod of the spring-loaded optical commutator drive system:

$$\Delta L = \frac{F^2}{16 p^2} \cdot L \cdot D(\alpha) e^{2 \cdot i \cdot \omega \cdot t} \tag{21}$$

where

$$D(\alpha) = tg^2\left(\frac{\alpha}{2}\right) + 3 + \frac{1}{\alpha}\left[(2\cos\alpha + 1) tg\frac{\alpha}{2} - 2\sin\alpha \right]$$

Next, an expression can be obtained for the displacement of the upper end of the rod of the spring loaded drive system or the upper end of the semitransparent mirror of the optical switch.

For this case, we will have [5]:

$$\Delta L_1 = \frac{F(t)^2 L}{32 P^2} \left[tg^2\frac{\alpha}{2} + 3 + \frac{4}{\alpha}(\cos\alpha + 1) tg\frac{\alpha}{2} - \frac{4}{\alpha}\sin\alpha \right] e^{2i\omega t} \tag{22}$$

$$\Delta L_2 = \frac{F(t)^2 L}{32 P^2} \left[tg^2\frac{\alpha}{2} + 3 - \frac{2}{\alpha} tg\frac{\alpha}{2} \right] e^{2i\omega t} \tag{23}$$

Taking into account (22) and (23) in (18), the expression describing the displacement of the semitransparent mirror is obtained as

$$\Delta L = \frac{F(t)^2 \cdot L}{16 P^2} \cdot D(\alpha) \cdot e^{2i\omega t} \tag{24}$$

Considering that $F(t) = F \cdot e^{i\omega t}$, find:

$$F(t) = 4 \cdot P \sqrt{\frac{\Delta L}{L \cdot D(\alpha)}} = 2mg \sqrt{\frac{\Delta L}{L \cdot D(\alpha)}} \tag{25}$$

where ΔL – displacement of the top end of a rod or translucent mirror.

Similarly, by imposing such particular solutions, one can obtain a formula for the external action $F(t)$ for the general case of transverse vibrations.

To determine the greatest transverse deflection of the bar $V_{\max}$, we will use the condition for fixing the plate. As noted, the function $V(x)$ reaches its maximum value when $X = L/2$, then:

$$V_1\left(\frac{L}{2}\right) = V_2\left(\frac{L}{2}\right) = V_{MAX} = \frac{F(t)}{4P} \cdot L \cdot D_1(\alpha) \tag{26}$$

where

$$D_1(\alpha) = \frac{2}{\alpha} \cdot tg\left(\frac{\alpha}{2}\right) - 1$$

Excluding the value of the external action from relation (26), we represent the largest transverse deflection in a different form:

$$V_{MAX} = D_1(\alpha) \cdot \sqrt{\frac{L \cdot \Delta L}{D(\alpha)}} \tag{27}$$

Also, it can be shown that:

$$\Delta L = \frac{D(\alpha)}{D_1^2(\alpha)} \cdot \frac{V_{MAX}^2}{L} = \frac{F(t)}{4p} \cdot \frac{D(\alpha)}{D_1(\alpha)} \cdot V_{MAX} \tag{28}$$

$$F(t) = 4p \cdot \frac{V_{MAX}}{L \cdot D_1(\alpha)} = 4p \frac{D_1(\alpha)}{D(\alpha)} \frac{\Delta L}{V_{MAX}} \tag{29}$$

Thus, all mathematical expressions for the dynamic parameters (such as the deflection equations $V(L)$, external force $F(t)$ and displacement of the upper end ΔL) of the spring-loaded system from the parameters of the elastic plate (L – length, b – width, h – thickness and m – masses of the elastic plate with a semitransparent mirror) of the optical commutator drive.

References

1. Maharramov VA, Gasanov M.G. About one principle of commutation of information flows. *Problems of Information Technology*, Baku, 2018. No.1, pp. 27-35.

2. Hasanov M.H. Multi-channepiezoelectric switch of adaptiveoptical networks. *The International science-technical journal Herald of the Azerbaijan Enginering Academy*. Baku, 2017. №4. pp. 107-112.

3. Ismailov T.K., Magerramov V.A. Scanning device, Auto. Svid. No. 1283698 A2 of the USSR, B.I., No.2. MKI G02 B26 / 10. 1987.

4. Timoshenko S. P. Oscillation in engineering. Moscow: Fizmatgiz. 1967. 444p.

5. Maharramov V. A. Technique of infrared observations of space objects (Fundamentals of theory and calculation). Baku. Elm. 1999. 336 p.

ABOUT RELATIONSHIP BETWEEN THE SIGNAL POWER, NUMBER OF M-QAM POSITIONS AND NOISE IMMUNITY IN BROADBAND WIRELESS ACCESS SYSTEMS

Isa Mammedov,
Azerbaijan Technical University, Baku, Azerbaijan,
isamamedov@bk.ru

Ilham Afandiyev,
State Management of Radiofrequencies of Ministry of Transport, Communication and High Technology, Baku, Azerbaijan,
ilham.afandiyev@gmail.com

DOI: 10.36724/2664-066X-2020-6-2-24-28

ABSTRACT

Is studied the effect of measurement error on the accuracy of selecting the modulation type in the transmitter of the base station. The article discusses changes in the statistical characteristics of the measured signal as it passes through the stage of the feedback loop of the system of the LMDS type. Probabilistic characteristics of pilot-signal are determined at the output of this loop. The aim of the work was to find a compromise between the type of modulation and the power of the BS transmitter to maintain the transmission faithfulness within the given limits in the forward channel of an interactive wireless broadband radio access system of the LMDS. In this system a transition is made from one type of modulation to another in order to maintain the noise immunity of the system within the admissible limits. An adaptive controlling method of modulation type makes it possible to obtain an energy gain in the forward channel of the system.

It is useful to determine the type of modulation by measuring the current value of the signal-to-interference ratio at the base station (BS) receiver. For this purpose a pilot signal is transmitted on the reverse channel of the system. This signal, passing through the turbulent medium, undergoes attenuation, and therefore at the input of the BS receiver we have a random process. Moreover, the distribution law of this process can be different and is determined by the communication channel model. The problem consisted in determining the necessary probabilistic characteristics of the output process by using the system parameters and probabilistic characteristics of the input random process. For this purpose the cumulants of the input random process and the random process at the output of the linear inertial system are determined. An expression for the probability density of the random process at the output of a linear inertial system is obtained.

The graphics of the error probability on the energy parameter at 16-QAM and 64-QAM type of modulation are constructed. The influence of the measurement error on the accuracy of the choice of the modulation type in the transmitter of the BS is studied. The limits of the change in the energy parameter are defined graphically, under which the modulation type changes to ensure a given error probability. It is determined, that the system is more critical to the measurement error at high admissible error probability, i.e. at high error probabilities, small errors in the measurement of the signal-to-noise ratio make it necessary to transition to a more noise-immune modulation mode.

KEYWORDS: *broadband wireless access system, base station, amplitude-phase modulation, power control, cumulant, adaptive selection of the modulation type*

Information about authors

Isa Mammadov, *Azerbaijan Technical University, professor, Baku, Azerbaijan*

Ilham Afandiyev, *State Management of Radiofrequencies of Ministry of Transport, Communication and High Technology, Chief Engineer, Baku, Azerbaijan*

1. Problem Statement

In order to provide the population with various types of information and to solve the "last mile" problem, integral telecommunication technologies are used, the varieties of which are wireless broadband radio access systems such as LMDS (Local Multipoint Distribution Systems) and MVDS (Multipoint Video Distribution Systems). These systems are high-speed and are built according to the cellular principle [1].

Various modulation methods have been proposed in LMDS systems [2]. Moreover, in the same base station transmitter (BS), different types of modulation are used, depending on the distance to the subscriber – for distant subscribers, a more noise-resistant type of modulation is used. Such a transition is carried out in order to maintain the system's noise immunity within acceptable limits. Typically, the signal strength decreases as distance to receiver increases. Therefore, in the named system, QPSK modulation is used for distant users, and for near ones it is replaced by M-QAM modulation.

Signal attenuation is random, and the known models of radio signal propagation make it possible to give only conjectural estimates of signal level at the receiving point. Therefore, changing the type of modulation, based on the distance to subscriber station, cannot give the desired result from the point of view of ensuring the necessary transmission fidelity. A quick assessment of the signal level in BS and the method of adaptive selection of the type of modulation and power control over BS transmitter channels may be the most acceptable option to ensure necessary transmission fidelity.

In mobile communication systems, open and closed loop power control methods are used to solve the far-close problem. Also, circuits and algorithms for power regulation in them are drawn up. The reference signal for power control is the pilot signals emitted by the subscriber transmitters.

The aim of this work is to find a compromise between the type of modulation and power of BS transmitter to maintain fidelity of transmission within the specified limits in forward channel of interactive system of wireless broadband radio access of LMDS type.

2. Controlling the type of modulation in broadband radio access systems

The power control in the forward channel is of particular importance, since at high power the BS transmitter interferes with other cells and sectors [3]. This adjustment helps reduce forward link interference.

Signal attenuation depends on various factors and the use of a certain type of modulation depending on the distance may not be beneficial due to energy considerations and a decrease in the transmission rate when using the appropriate type of modulation. Therefore, it is of interest to determine the type of modulation by measuring the current value of the signal-to-noise ratio in the BS. Such an adaptive method for controlling the type of modulation will provide an energy gain in the forward channel.

The stated task belongs to the class of systems management. Control is a purposeful impact on the control object to maintain certain parameters within the required limits. System identification, state estimation and control are the main typical tasks of systems control theory. It can be deterministic or stochastic. Typically, external disturbances affect the operation of the control system. If you do not take into account the influence of these interferences, then the control system is considered deterministic. Taking into account the noise and their statistical features, the control system is considered as stochastic [4]. Stochastic control performs the task of optimal control of the system under the influence of noise on the control and measuring units.

Pilot signal emitted by subscriber station, passing through a turbulent medium, undergoes attenuation, and therefore at the input of BS receiver we have a signal:

$$S(t) = A(t)\cos[\omega_0 t + \varphi_0 + \varphi(t)].$$

Here ω_0 – frequency, φ_0 – initial phase, $A(t)$ – amplitude, $\varphi(t)$ – random phase of the pilot signal at the input of the demodulator. The amplitude and phase of the measured signal are random in this case. Moreover, the laws of their distribution can be different and are determined by the communication channel model [5]. From the given distribution models of the signal value, the distribution of the signal amplitude can be determined. For example, if during slow fading the distribution of the signal value obeys a lognormal law, then the signal amplitude is described by the Rice distribution law [6]. A pilot signal arrives at the detector's input, the amplitude of which obeys one of the above laws.

3. Change in the statistical parameters of the measured signal when it passes through the control circuit stages

Pilot signal is fed to the demodulator input. Pilot signal demodulator can be represented by the following block diagram (Fig. 1). The task is to determine required probabilistic characteristics of the output process with known parameters of system and probabilistic characteristics of input random process. In communication theory, filters belong to the class of linear inertial systems. A system is called linear if it obeys of superposition principle. A linear inertial system, at the input of which there is a random process $\xi(t)$, starting from the moment t = 0, is described by a fluctuation differential equation [4]. Exact solution to this equation obtained for a Gaussian random process.

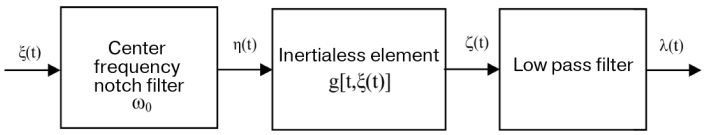

Figure 1. Block diagram of the measuring signal demodulator

We assume that the input random process is stationary in broad sense. Methods for determining the probability density at output of a linear inertial system are known if probability density of input random process is known. Based on the known probability density of input random process, its cumulants are found [4, 6]:

$$æ_{\xi k} = \left.\frac{d^k \psi_\xi(v)}{dv}\right|_{v=0}, \qquad k = 1, 2, 3, ...$$

Here

$$\psi_\xi(v) = ln\,\theta_\xi(v) = ln\left[\int_{-\infty}^{\infty} w_\xi(x) e^{ivx} dx\right],$$

$w_\xi(x)$ – one-dimensional probability density of input random process $\xi(t)$, $\theta_\xi(v)$ – its characteristic function.

After calculating the cumulants of the input random process, the transfer function of the linear inertial system is determined. Transfer functions of filters are given in the literature [4, 6]. Let us assume that the impulse response of this system is expressed by the formula [4, 6]:

$$g(t) = \alpha e^{-\alpha t}. \qquad \alpha = \frac{1}{RC} \tag{1}$$

We calculate the cumulants of output random process $\eta(t)$, for which we use impulse response of this linear system and expression [4, 7]:

$$\frac{æ_{\eta k}}{æ_{\xi k}} = \int_0^\infty \left[\int_0^\infty g(t-u)g(u)du\right]^k dt \Big/ \int_0^\infty [g(t)]^k dt. \tag{2}$$

Integrating in (2), taking into account (1) for values $t \geq 0$ and $\alpha > 0$ (which correspond to conditions of our problem), we find:

$$æ_{\eta k} = \frac{\frac{\alpha^k}{4^k}\int_0^\infty e^{-\alpha t} dt}{\frac{\alpha^{k-1}}{k}} æ_{\xi k} = \frac{æ_{\xi k}}{4^k}. \tag{3}$$

Taking into account the values of the cumulants of the input random process $\xi(t)$ 7] from (3) obtain:

$$\begin{aligned} æ_{\eta 1} &= \frac{m_{\xi 1}}{4}; \quad æ_{\eta 2} = \frac{m_{\xi 2} - m_{\xi 1}^2}{16}; \\ æ_{\eta 3} &= \frac{3\left(m_{\xi 3} - 3m_{\xi 2}m_{\xi 1} + 2m_{\xi 1}^3\right)}{64}; \\ æ_{\eta 4} &= \frac{m_{\xi 4} - 4m_{\xi 3}m_{\xi 1} - 3m_{\xi 2}^2 + 12m_{\xi 2}m_{\xi 1}^2 - 6m_{\xi 1}^4}{256} = \\ &= \frac{M_{\xi 4} - 3M_{\xi 2}^2}{256} \end{aligned}. \tag{4}$$

where $m_{\xi k}$ and $M_{\xi k}$ – respectively, initial and central moments of distribution of the input random process.

The approximation of the probability density of a random process at the output of a linear inertial system is carried out by the cumulants at the output of this system. We apply the Edgeworth series to approximate the probability density of output random process [4, 6]. The named series after rearrangement has the form [8]:

$$\begin{aligned} w_\eta(y) &= \frac{1}{2\pi} e^{-y^2/2} \times \\ &\times \left[1 + \frac{æ_{\eta 3}}{3}\left(2,7y^6 - 20y^4 + 34y^2 - 6y - 5\right) + \right. \\ &\left. + \frac{æ_{\eta 4}}{6}\left(4y^4 - 12y^2 + 3\right) + \frac{æ_{\eta 5}}{30}\left(8y^5 - 40y^3 + 3y\right) + \cdots\right] \end{aligned}, \tag{5}$$

where $H_n(y)$ – Hermite polynomials defined by the formulas [4]:

$$H_n(y) = (-1)^n e^{y^2} \frac{d^n e^{-y^2}}{dy^n}, \qquad n = 0,\ 1,\ 2, \cdots$$

For small values of high-order cumulants, we use only the first two terms in (5). Then initial moments of the first, second and third order participate in the approximated probability density of random process at filter output.

Suppose the pilot signal amplitude obeys a Rayleigh distribution. Then for the input random process we define:

$$æ_{\xi 1} = m_{\xi 1} = \sigma_\xi \sqrt{\frac{\pi}{2}};\ æ_{\xi 2} = m_{\xi 2} - m_{\xi 1}^2 = \frac{4-\pi}{2}\sigma_\xi^2;$$

$$m_{\xi 2} = 2\sigma_\xi^2;\ æ_{\xi 3} = M_{\xi 3} = (\pi - 3)\sqrt{\frac{\pi}{2}}\sigma_\xi^3;$$

$$æ_{\xi 4} = M_{\xi 4} - 3M_{\xi 2}^2 = 0{,}05\sigma_\xi^4.$$

The cumulants of output random process are determined using (4):

$$æ_{\eta 1} = \sigma_\xi \sqrt{\frac{\pi}{32}};\ æ_{\eta 2} = \frac{(4-\pi)\sigma_\xi^2}{32};$$
$$æ_{\eta 3} = \frac{M_{\xi 3}^2}{64} = \frac{(\pi - 3)}{64}\sqrt{\frac{\pi}{2}}\sigma_\xi^3;\ æ_{\eta 4} = \frac{0{,}05\sigma_\xi^4}{256}.$$

Then from (5) find:

$$\begin{aligned} w_\eta(y) &\approx \frac{1}{2\pi} e^{-y^2/2}\left[1 + \frac{(\pi - 3)}{64}\sqrt{\frac{\pi}{2}}\sigma_\xi^3 \times \right. \\ &\left. \times \left(2,7y^6 - 20y^4 + 34y^2 - 6y - 5\right)\right] \end{aligned}. \tag{6}$$

The resulting expression describes the distribution of pilot signal amplitude at output of feedback loop filter with amplitude fluctuations according to Rayleigh law in the communication channel. This distribution is not symmetric and, for non-symmetric distributions, Edgeworth series is not the best option. Second term in the middle bracket on the right side of expression (6) is a polynomial. Therefore, it would be convenient here to use Pearson polynomials for approximation.

To determine probabilistic characteristics of a random process $\zeta(t)$ (Fig. 1), it is necessary to know the characteristics $g[t,\eta(t)]$ of a nonlinear element (detector), where $\eta(t)$ – input, $\zeta(t)$ – output random processes, function $g(\cdot)$ is determined by system parameters. This function is deterministic. We assume that sum of measured signal and fluctuation noise acts at the detector input:

$$\eta(t) = S(t,\varphi) + n(t), \tag{7}$$

where *n(t)* – Gaussian random process with zero mathematical expectation.

The one-dimensional probability density of two independent random processes sum is determined by well-known formula.

Based on the arguments of literature [6], taking into account (7), we find the probability density of a random process at the detector output:

$$w_\zeta(z_1,t_1) = w_\eta\left(\frac{z_1+y_0}{R_i},t\right) + \delta(z_1)\int_{-\infty}^{y_0} w_\eta(y_1,t_1)dy_1;$$

$$z_1 > 0$$

Here $w_S(x_1,t_1)$ and $w_n(y_1,t_1)$ – p obability density of processes $S(t,\varphi)$ and $n(t)$ respectively, $\delta(z_1)$ – lta function.

4. nfluence of measurement accuracy on the system noise immunity

The literature investigates noise immunity of communication systems with amplitude-phase modulation. The probability of an error under the action of only fluctuation noise was determined [9]:

$$p_{ош}\left(h_б^2\right) = \frac{2\left(1-\frac{1}{\sqrt{M}}\right)}{log_2 M} Q\left(\sqrt{\frac{3log_2 M}{2(M-1)}h_б^2}\right), \tag{8}$$

where M – number of QAM signal positions, $Q(\cdot)$ – error function, $h_б^2 = \frac{E_б}{N_0}$, N_0 – noise intensity, $E_б$ – the energy of one bit, determined by the formula: $E_б = T_б P_c$, P_c – average signal strength, $T_б$ – information bit duration: $T_б = T_{эс}/log_2 M$, $T_{эс}$ – elementary duration: $T_{эс} = \frac{1}{\Delta F_c}$, ΔF_c – signal spectrum width.

It is shown that real broadband interference can be represented as white Gaussian noise and, at the same time, with some accuracy, the energy parameter can be determined from the noise immunity as the ratio of the average signal energy to the spectral density of the noise and the above interference $h_{б\Sigma}^2$ [10]. It is also possible to determine with some accuracy the probability of error under the action of the above-mentioned interference by the formula obtained for signal reception against the background of fluctuation noise. For this, in formula (8) we replace $h_б^2$ by $h_{б\Sigma}^2$

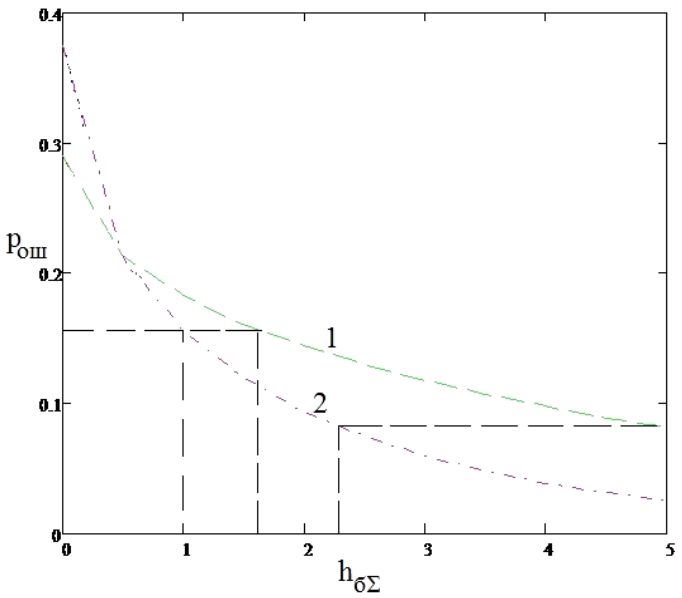

Figure 2. Dependences of the error probability on the energy parameter $h_{б\Sigma}^2$:
1 – if a signal is received when UWB and jitter noise for 64-QAM;
2 – in case of receiving a signal during action UWB interference and fluctuation noise for 16 QAM

We have constructed graphs of the dependence of the error probability $p_{ош}$ on the energy parameter $h_{б\Sigma}^2$ for 16-QAM and 64-QAM in the case of ultra-wideband interference and taking into account fluctuation noise (Fig. 2). It follows from the graphs that, with a high permissible error probability, a small change in the signal-to-noise ratio makes it necessary to switch from one mode to another - a more noise-immune modulation mode. For example, at $p_{ош}$ = 0.16 with an increase $h_{б\Sigma}^2$ of 1.6 times, it is necessary to change the modulation mode, while at $p_{ош}$ = 0.08, such a change must be carried out with an increase $h_{б\Sigma}^2$ of 2.27 times. Therefore, in the first case, the measurement system is more sensitive to measurement errors.

Conclusions

Changing the type of modulation, based on distance to subscriber station, cannot give the desired result in terms of ensuring necessary transmission fidelity. Adaptive choice of type modulation and power control over the BS transmitter channels by real-time estimation of signal level in BS may be the most acceptable option to ensure necessary transmission fidelity.

A pilot signal, passing through a turbulent propagation medium, becomes a random process. For the accuracy of determining power value or signal-to-noise ratio, the change in statistical parameters of this random process at output of main stages in

closed feedback loop was studied. With a high permissible error probability, small errors in measuring signal-to-noise ratio make it necessary to switch from one mode to another – more noise-immune modulation mode.

References

1. http://www.rrl.com.ua/ru/ fo/our/codec/02. 03.06.2016.

2. Hakegard, J.E. Coding and Modulation for LMDS and Analysis of the LMDS Channels. *Journal of Research of the National Institute of Standards and Technology*, 2000, vol. 105, no 5, pp. 721-734.

3. Bolshov O.A. and Perminov, P.A. Development of feedback channel in the system of wireless broadband access (Cellular Television). *Special technique and Communication*, 2010, no. 1, pp. 37-45.

4. Levin, B.R. and Shvarts, V. *Veroyatnostniye modeli i metodi v sistemakh svyazi i upravleniya* [Probabilistic models and methods in communication and control systems]. Moscow: Radio i svyaz. 1985.

5. Evstratov, A.Q. and Pustovoytov, E.L. Calculation of the influence of the interfering radio signal on the receiver of the digital radio communication system under the known distribution laws of fast and slow fading of useful and interfering radio signals. 2014. *T-Comm*, no.5, pp. 50-55.

6. Levin, B. R. *Teoreticheskiye osnovy statisticheskoy radiotekhniki.* Kniqa 1 [Theoretical bases of statistical radio engineering. Book 1]. Moscow: Sovetskoye radio. 1974.

7. Mamedov, I.R. and Aliyev, Z.B. Probabilistic description of the amplitude of the pilot signal at the output of a closed feedback loop. *Telecommunications*, 2012. No. 2, pp. 39-42.

8. Mamedov, I.R. and Aliyev, Z.B. Influence of the accuracy of power adjustment on the noise immunity of the feedback link of mo-bile communication. *T-Comm*, 2014, no. 12, pp. 59-61.

9. Cho, K. and Yoon, D. On the General BER Expression of One- and Two-Dimensional Amplitude Modulations. *IEEE Trans. on Communications*, 2002, vol. 50, July, no. 7, pp. 1074-1080.

10. Aronov, D.A. Estimation of the error probability per bit of transmitted information in the presence of noise and modulated interference. 2007, *Telecommunications*, no. 11, pp. 56-59.

ENHANCING 5G WITH MICROWAVE

Git Sellin (Executive Editor**)**
Maria Edberg (Editor)
Magnus Berggren, Mikael Coldrey, Jonas Edstam, Dennis Eriksson, Jonas Flodin,
Jonas Hansryd, Andreas Olsson, Mikael Ohberg, *Ericsson, Stockholm, Sweden*
Dimitris Siomos (Co-written article), *Deutsche Telekom*

Ericsson White Paper

ABSTRACT

To meet the rapid deployment of 5G around the globe, it is evident that a variety of transport solutions are required in order to fulfill the needs of communications service providers. The international rollout of 5G is progressing much more quickly than anticipated and the necessity for high capacity backhaul and fronthaul has never been more apparent. Suburban and urban high capacity sites in 2022 will require capacities of up to 2 and 10Gbps respectively, while towards 2025 we will see examples of sites stretching between 5 and 20Gbps. Microwave is already well positioned to support all backhaul capacity needs using standalone E-band or multi-carrier solutions. In regards to fronthaul, microwave can act as a complement to fiber for antenna site capacities in a range of 10Gbps in 2019 and 25Gbps by 2022.

Now that commercial 5G services have gathered a strong global momentum, the dust settles on future spectrum use. Some backhaul frequency bands will eventually be transitioned to 5G access use, such as 26GHz in Europe. In contrast, the E-band and 32GHz band are acknowledged as essential for the backhaul of 5G. The solutions which are viable for each service provider and country are dictated by microwave spectrum availability, which in turn impacts both capacity and the total cost of ownership. In order to enable higher capacities in both traditional spectrum and E-band, access to wider bandwidths is important. Without this, more complex and spectrum-efficient solutions are required. MIMO is an important enabler for countries with limited spectrum availability to reach high capacity links of 1Gbps and beyond. By using MIMO and E-band radios,

Deutsche Telekom and Ericsson were able to smash the 100Gbps barrier during a trial in Athens, Greece. With optimal antenna arrangement, the trial achieved 139Gbps over 1.5km, with high availability and low latency. Such microwave links will be ideal as cost- and time-efficient complements to optical fiber for closure and redundancy of metro and core fiber rings, fiber extension applications, campus and enterprise connections and backups to existing high-capacity fiber links. As a result of technological developments, we expect that the first 100Gbps links will be deployed in 5 to 8 years, depending on the market demands. After almost a decade of experience in commercial E-band deployment, we have gained a number of insights to assist in E-band's future usage. For example, we foresee an increased use of E-band for longer hops, even if that means accepting a slightly lower availability. The widespread use of E-band increasingly supports our prediction that E-band will account for 20 percent of all new microwave links by 2025. It is evident that microwave is well prepared for the network evolution of 5G and beyond.

KEYWORDS: *E-band, MIMO for microwave, 100Gbps barrier, 5G*

This article was written in collaboration with Deutsche Telekom – one of the world's leading integrated telecommunications companies, with some 178 million mobile customers, 28 million fixed-network lines, and 20 million broadband lines in more than 50 countries. They provide fixed-network/broadband, mobile communications, Internet, and IPTV products and services for consumers, and information and communication technology (ICT) solutions for business and corporate customers.

Handling the capacity evolution

As seen in the June 2019 edition of the Ericsson Mobility Report, the 5G rollout is happening quicker than expected. The LTE and 5G New Radio (5G NR) expansion will continue in terms of both capacity and coverage. LTE coverage will reach 90 percent and 5G coverage 45–65 percent (depending on deployments in the existing LTE band) by 2024 across the globe.

The increase in backhaul capacity per site when introducing 5G NR depends on several considerations, such as technology (e.g. MU-MIMO), 5G NR spectrum (low, mid and high band) and potential underlying small cells within its coverage area. The upper table in Figure 1 is a forecast of the backhaul capacity per site, with the predictions for 2022 and towards 2025 that support the rollout of 5G NR.

Backhaul capacity per site

	2019 Low – high cap. sites	2022 Low – high cap. sites	Towards 2025 Low – high cap. sites
Urban	250Mbps – 2Gbps	450Mbps – 10Gbps	600Mbps – 20Gbps
Suburban	100Mbps – 500Mbps	200Mbps – 2Gbps	300Mbps – 5Gbps
Rural	50Mbps – 150Mbps	75Mbps – 350Mbps	100Mbps – 600Mbps

Fronthaul capacity per site

	2019	2022	Towards 2025
Antenna site	up to 10Gbps	up to 25Gbps	up to 100Gbps

Source: Ericsson (2019)

Figure 1. Capacity forecast

The figures for 2019 show a slight increase for both urban sites and suburban high capacity sites due to LTE capacity upgrades in the networks. The low capacity figures represent around 80 percent of all sites, while the high capacity figures represent only a small percentage. Suburban and urban high-capacity sites in 2022 will require capacities up to 2 and 10Gbps respectively, while towards 2025, we will see examples of sites stretching between 5 and 20Gbps respectively. Microwave is well positioned and can already today support all these capacity scenarios, using standalone E-band or multi-carrier solutions within the band and/or across several bands, such as E-band in combination with 18GHz.

Fronthaul is the connection between the digital unit and the antenna, which are the Common Public Radio Interface (CPRI) and evolved CPRI (eCPRI) interfaces, as seen in Figure 2. These interfaces require higher bandwidths and very low latency compared to Next Generation (NG) or F1 interfaces. Microwave is a complementary technology for fronthaul, when fiber is not a viable solution.

The capacity per antenna site is the capacity of the connection to the digital unit, either on the same site or at a C-RAN site. An antenna site can also be an offshoot from a D-RAN site, typically as a small cell or street macro deployment. Microwave can be used at the antenna site when capacities are in the range of 10Gbps in 2019 and 25Gbps towards 2022. The introduction of eCPRI will enable the use of standard packet E-band radios. E-band can already support low capacity antenna sites, with the potential to reach beyond 100Gbps in the future; other fronthaul use cases might also be applicable.

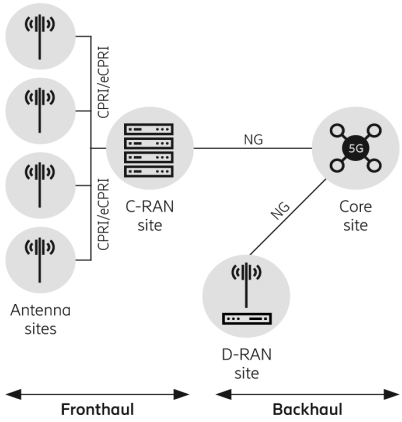

Figure 2. Simplified RAN architecture

Figure 1 states the expected future capacities, but it is important that we know how service providers are currently handling the capacity evolution with microwave links. We have examined two very different regions – the Scandinavian countries and India. As a Scandinavian service provider exemplified by Hi3G in this paper, both traditional bands (6, 7, 8, 10, 11, 13, 15, 18, 23, 26, 28, 32, 38 and 42GHz) and E-band are available, while in India, only 7, 13, 15, 18 and 23GHz can be used. Moreover, in Sweden, link-by-link licensing is normally used (with a few exceptions) for both traditional bands and E-band, while service providers only pay a small fee per carrier, irrespective of the frequency band or channel bandwidth.

In Denmark, traditional bands and E-band are link-by-link and the spectrum fee is proportional to the channel bandwidth.

In India the spectrum is block licensed per circle, per 28MHz channel. All these differences result in totally different strategies and solutions for microwave links in their networks.

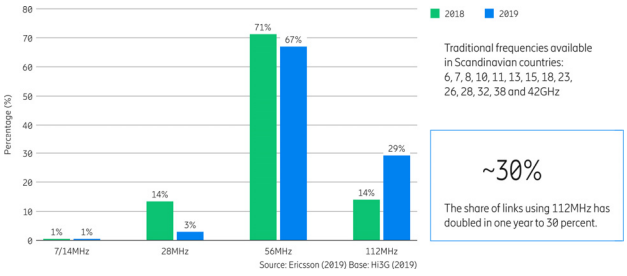

Figure 3. How a Scandinavian service provider expands capacity in traditional bands

Figure 3 shows a clear trend in Scandinavian countries when comparing 2018 with 2019. Moving from narrow channels to 112MHz channels, with or without XPIC, means a migration to more than 1Gbps using one or two carriers on traditional bands. For this particular Scandinavian service provider, 29 percent of all traditional links are 112MHz in 2019. Combined with the introduction of E-band links in their network, as seen in Figure 4, we can see that 70 percent of E-band links are designed for 3Gbps or more. By comparing the E-band strategies of

Sweden and Denmark, there is a majority of 250 and 500MHz links for Denmark, with wider channels for Sweden. This is largely due to the different spectrum fee strategies in each country.

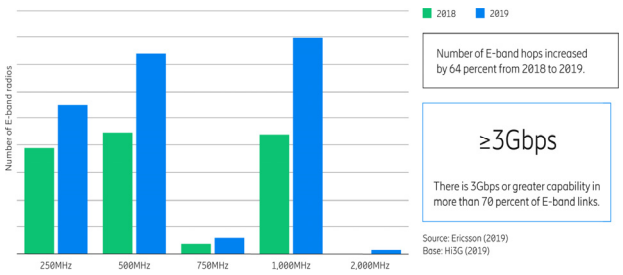

Figure 4. A Scandinavian service provider expanding capacity with E-band

In comparison, an Indian service provider only has a few bands to use and only 28MHz channels. They need to use multi-carrier solutions to meet high capacity links of 1Gbps and beyond, which means more complex site solutions, such as quadruple carriers and using MIMO. It is evident that the spectrum and availability of wider channels, including E-band, simplifies the migration towards increased capacity in a network with single carrier and dual carrier multi-band solutions.

The latest on spectrum

In country after country, 5G networks are being switched on and by 2024 they are expected to carry 35 percent of the global mobile data traffic.1.

New spectrum in high, mid and low frequency bands are being planned and awarded in an ever-increasing number of nations. Subsets of the new bands are often made available on a national level, to stepwise transition existing users (such as satellite, broadcasters, fixed wireless or others) from the band. In addition, all 3GPP bands in use for current mobile generations will eventually be considered for 5G services. An even faster rollout of 5G coverage can be supported by deployments of 5G in the same spectrum as 4G, enabled by a technological advancement known as spectrum sharing.

Microwave backhaul is used extensively in many frequency bands above 6GHz and will remain an essential transport medium for 5G. Some of these bands will increase in backhaul use, while others will eventually transition to 5G NR access. The timing of the transition will vary, as the best use of each band will change over time in different countries. In addition to the 5G spectrum plans of pioneering countries, the International Telecommunication Union's (ITU) World Radiocommunication Conference (WRC-19) in November 2019 will identify which bands in the 24-86GHz range suit 5G.

The us takes the lead in high band 5G

The ranges 24.25-29.5GHz and 37-43.5GHz are specified by 3GPP for 5G NR. The United States is leading the efforts on 5G NR use in high bands, with 4GHz of total bandwidth being released in the 24, 28, 37 and 39GHz bands. Other leading countries are Korea, which has released 2.4GHz in the 28GHz band, and Japan, which has released 1.6GHz in the 28GHz band. In Europe, the 26GHz band (24.25-27.5GHz) is the pioneering high band, with some countries expected to release a 1GHz subset as a first phase.

Europe is also interested in the 42GHz band, since the 38GHz band is too heavily used for microwave backhaul and also intended for satellite use. Work to harmonize the 42GHz band for 5G is expected to start immediately after WRC-19. China has indicated interest in the 24.75-27.5GHz band and the 37-43.5GHz range. A global overview of decisions and indications for the 26 and 28GHz bands is shown in Figure 5.

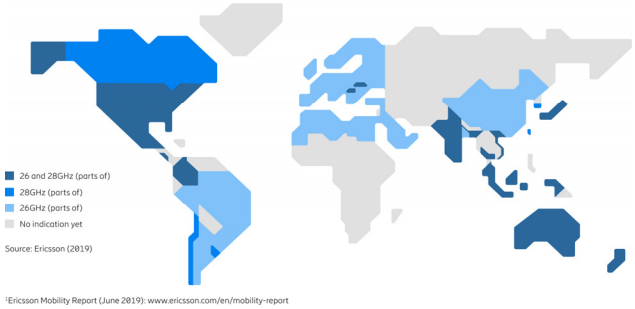

Figure 5. 26 and 28GHz bands being decided or considered for 5G NR

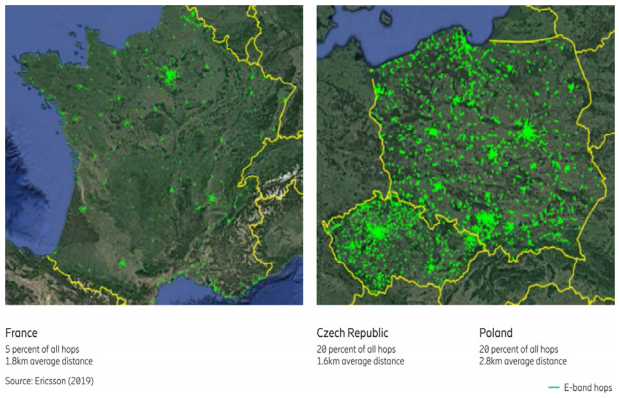

Figure 6. The momentum of E-band backhaul

Essential frequency bands for backhaul

The E-band (71-76GHz paired with 81-86GHz) is becoming an essential backhaul band of high global alignment. Its use has grown rapidly over the last couple of years, especially in countries with an attractive spectrum license fee. For example, in Poland and the Czech Republic, about 20 percent of all hops are now in E-band (Figure 6). In preparation for 5G, transport networks will be upgraded to support higher capacities. Fiber penetration will increase, and the E-band is the widely recognized frequency choice for 5G transport in urban and suburban areas.

This will facilitate the transition of backhaul from bands now being designated for 5G NR use, such as 26GHz in Europe. The E-band has been studied for 5G NR access use, but this no longer has any support. However, it has been acknowledged as essential for backhaul use. The 32GHz band (31.8-33.4GHz) has also been deemed unsuitable for 5G NR, and instead it is a strong candidate to become a global backhaul band.

Scattered view and use of the 60GHz band

The backhaul usage in the 57-66GHz band is very limited. The band's status has been immature, with subsets licensed for backhaul in some countries, while in other countries it is designated for license-exempt technology agnostic use. The whole band is unlicensed in the United States, with rules to limit the probability of interference for wireless configurations with everything from omni to high directivity antennas.

In Europe, the rules were changed in June 2019 to allow similar license-exempt use as the United States. These rules are expected to keep the probability of interference between applications low. However, high reliability usage is not recommended, as high quality cannot be guaranteed in license-exempt bands.

The 66-71GHz range has been studied for 5G ahead of the WRC-19 and is generally seen as well suited. However, there are some different national and regional opinions on the licensing and use of the band. For example, 64-71GHz was added to form a 57-71GHz band for unlicensed use in the United States. In Europe, there is desire that the 66-71GHz band, while supported for 5G, should also be made available for other wireless access technologies on an equal basis. 3GPP is expected to specify 5G NR for the 57-71GHz band in a few years.

Looking to the future, discussions have now started on new 5G bands in the 6-24GHz range. For example, China is planning to study the 6GHz band for licensed 5G. Frequency bands below 10GHz are essential for long-range backhaul. However, these are sparsely deployed and, as a result, there is locally unused spectrum. The opportunity to introduce license-exempt, technology neutral, wireless access is being studied in both the United States and Europe for parts of the 6GHz band, with the requirement that there is no harmful interference for backhaul use. 3GPP also specifies the 6GHz band for unlicensed NR.

Spectrum is a finite resource and more efficient use will be needed in the future. There are large variations in the use of backhaul bands in different locations, countries and regions, depending on the demand and the most valuable use of spectrum in each location. In the future, we will see some nations decide to use a band for 5G NR, while others use it for backhaul.

Some countries might even decide to use a band for 5G NR in urban areas, but for backhaul in rural areas. Although the use of microwave backhaul is increasing globally, the need for much more bandwidth per hop is the main spectrum challenge. Wide frequency bands supporting short, mid and long-range backhaul are essential, along with continued technological innovations. The possibility to use more spectrum by sharing it with other radio services could also be a future opportunity.

Lessons learned from a decade with e-band

Many operators are facing a need to update their backhaul network to meet the capacity requirements of a 5G rollout. The RAN capacities in a 5G network, especially in urban/suburban environments, increase the need for backhaul equipment capable of handling multi-gigabit traffic in acost-efficient way. With limited spectrum in the traditional frequency bands, the attention directed towards E-band is constantly increasing. The technology has been successfully proven in several countries for a number of years and will increasingly be needed to boost capacity in urban sites, along with multi-band booster (MBB) combinations in suburban sites. As can be seen in Figure 7, the momentum of E-band is in full swing. In 2018 there were 14 times more E-band radios sold globally compared to 2011.

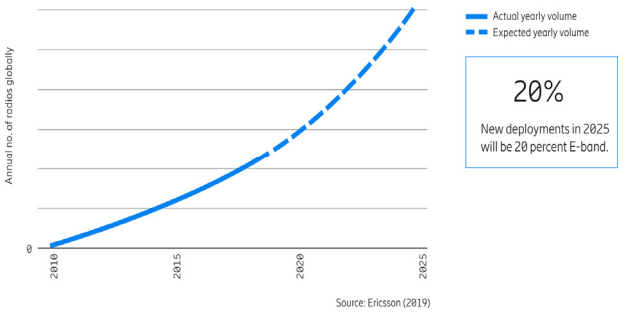

Figure 7. Growth of E-band radios from 2010-2018 and predicted for 2019-2025

As the worldwide 5G rollout drives the need for cost-efficient backhaul capacity and E-band becomes available in more countries, the curve is expected to become even steeper. With this continued growth in mind, 20 percent of new deployments are estimated to be E-band by 2025. From a decade of both standalone and multi-band E-band deployment, there are three main lessons to be drawn.

Reality matching predicted availability

For deployment of E-band radios in a network, the MBB concept is one of the key strategies. The obvious benefits are that it increases the capacity of an existing hop or stretches the hop length of the E-band. The trade-off in all of this is the availability of the E-band. Figure 8 shows the availabilities for an 18GHz radio and an E-band radio, measured over 12 months in Gothenburg, Sweden (Rain zone E, ITU-R 837-1).

The hop is a 7km long MBB configuration, using a combination of an 18GHz radio with a 28MHz channel and an E-band radio with a 125MHz channel. The 18GHz radio had consistent traffic during the 12-month period and the E-band radio remained at maximum modulation and capacity for more than 98 percent of the time. The E-band link contributed to the total capacity 99.93 percent of the time.

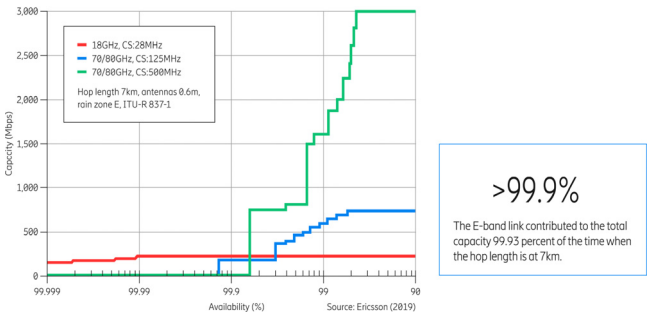

Figure 8. Availability and performance for a multi-band booster hop measured over 12 months

When using an E-band radio with a 500MHz channel, the corresponding values for the E-band's maximum modulation are just short of 98 percent, and the E-band is contributing close to 99.83 percent of the time. From a capacity perspective, it means that the hop never drops below 175Mbps and 99.93/99.83 percent of the time the E-band kicks in and boosts the hop with up to 17 times the capacity.

1. Longer hops win over high availability

One perceived drawback of any E-band deployment has been the idea of big limitations when it comes to hop length: that it is only applicable for one, maybe two kilometers. In Poland, where E-band penetration now exceeds 20 percent (as of May 2019), the service providers have chosen a method which allows for very long E-band hops. This distribution of hop lengths can be seen in Figure 9. Hops that are between 2 and 5km stand for 22 percent of the total, and as many as 11 percent of the hops are 6km or longer. In fact, 154 hops are 10km or even longer.

The distances where standalone E-band is used and where MBB hops begin to be introduced varies between service providers. Some start to deploy MBB at 3.5km and some wait until the distance is as long as 5km. The way to do this is to adjust the availability requirements of the E-band, in both standalone and MBB configurations.

Figure 10 shows 7 lengthy live hops, ranging from 4.1 to 12km in length (note: all are in different locations in Poland with different rain intensity and vendor equipment) and the corresponding availability figures achieved for each modulation. By stepping away from the historical requirement of 'five nines', these impressive lengths have been achieved. It is evident that E-band is a more viable solution for longer hops than previously expected and that Polish service providers have started to move towards a more packet-based approach to network planning, thus expanding the use of E-band radios.

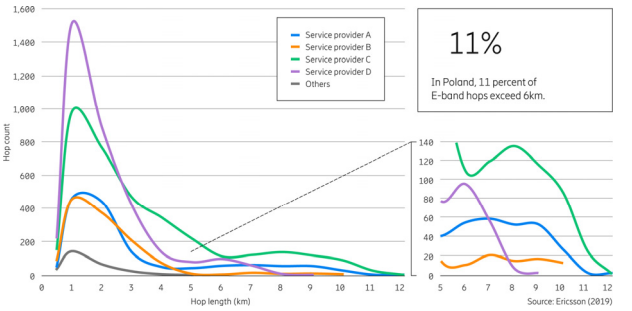

Figure 9. E-band microwave hops deployed in Poland, split by distance

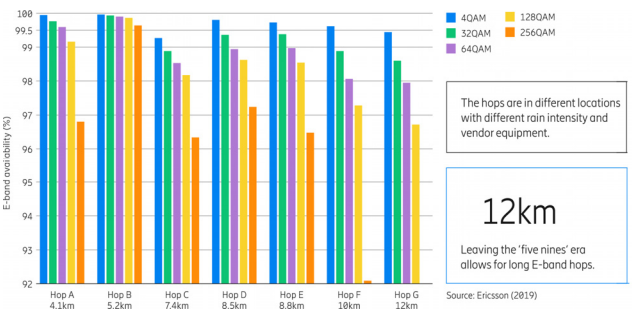

Figure 10. Live data for multi-band booster E-band hops in Poland, availability for various modulations

2. Accurate alignment is growing in importance

Point-to-point microwave links use high-gain antennas in the 30 to 50dBi range, corresponding to a half-power beamwidth (HPBW) of 5 and 0.5deg respectively. The lower gain limit is set by interference and frequency reuse, while the upper limit is set by practical limitations on alignment and stability. The gain distribution in different frequency ranges can be found in Figure 11. In the traditional bands (between 6 and 42GHz) the average gain distribution is in the 37 to 41dBi range, with the bulk well below 45dBi. Millions of such antennas have been installed. Only a small percentage of the installations have used very high gain antennas close to the upper 50dBi limit. It is understood that extra attention and skilled installers have been needed on a few links.

With the introduction of E-band, the distribution looks very different, with most links having an antenna gain above 45dBi (HPBW 1deg) and with an average as high as 48dBi. This means alignment skills are needed on many more links and the importance of stable masts also becomes more apparent. The main reasons for the high share of very high gain antennas in E-band are:

– Many E-band links deployed so far have replaced an existing link in a traditional band to save spectrum cost. With a pre-defined hop length, the gain needs to be maximized;

– in order to minimize the impact on availability at the higher frequency. The same gain can be achieved with half the antenna diameter when the frequency is doubled. With an antenna as small as 0.6m in diameter a gain of 50dBi can be achieved at E-band. This is the most popular size in traditional bands, and is consequently being selected also for E-band;

– The regulations in some markets require a relatively high minimum gain.

In a future with denser networks and shorter hops, along with increased radio output power, the E-band average gain will go down. This will simplify those types of installations. On the other hand, E-band will also be used for even longer hops than today. If the gain increases beyond 50dBi then self-alignment and mast sway compensation will be mandatory.

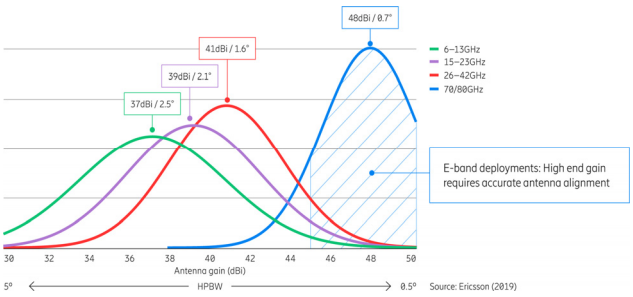

Figure 11. Antenna gain distribution per frequency range, deployments 2014-2018

Demystifying mimo for microwave

Multiple-Input Multiple-Output (MIMO) is a well-established antenna technology for enhancing spectral efficiency and/or reliability in wireless communication, and is being successfully used in 3GPP and Wi-Fi tech-

nologies. In a MIMO system, multiple antennas are deployed at both the transmitter and receiver side of a link.

The multiple antennas can be used for either:

1) i reasing the spectral efficiency (bps/Hz – bits per second and Hz) of the link by transmitting multiple data streams over the channel (also called spatial multiplexing) or 2) increasing the reliability of the link by exploiting the diversity gain introduced by the use of multiple antennas (also called spatial diversity).

A MIMO channel can be decomposed into multiple Single-Input Single-Output (SISO) channels over the same time and frequency. These channels are sometimes referred to as sub-channels of the overall MIMO channel. It is the use of these sub-channels in parallel over the same time and frequency channel that provides spatial multiplexing in MIMO.

For example, a properly designed MIMO system with 8 transmit and 8 receive antennas (8x8 MIMO) will have 8 sub-channels for spatial multiplexing.

In other words, the 8x8 system will have up to 8 times the capacity of a single antenna system. For example, assuming that 6 bits per data symbol (64 QAM) is used in an 8x8 MIMO system over an E-band signalbandwidth of 2.25GHz – the overall rate will be 6 (bits per symbol) x 8 (data streams) x 2.25 (GHz) = 108Gbps. Through this, MIMO acts as an enabler for reaching 100Gbps and beyond.

In general, there is a trade-off between spatial multiplexing and diversity gain, meaning that one typically chooses which to prioritize. For example, in microwave long-haul links, spatial diversity receivers are commonly used to combat multipath fading, therefore offering protection to critical backhaul links. In a spatial diversity system, the data information is conveyed over different sub-channels, which increases the link protection as it is unlikely that all sub-channels will fade at the same time. This also means that a spatial diversity system typically has increased availability of a certain data rate compared to a non-diversity system. In contrast to spatial diversity, a spatial multiplexing system instead uses all of the sub-channels to transmit multiple data streams in order to increase the spectral efficiency of the link. High spectral efficiency is important when spectrum is a scarce resource, which makes MIMO an attractive solution.

Principles of MIMO for microwave

The main intention in utilizing MIMO is in relation to multiple stream transmissions, in order to further enhance the spectral efficiency in microwave links. Spectral efficiency is enhanced by up to N times compared to a SISO system, where N is the MIMO order, limited by the number of antennas used in the MIMO system. In MIMO systems, it is possible to deploy any number of transmit and receive antennas, but a symmetric system is the most common, where the number of transmit antennas equals the number of receive antennas (NxN MIMO system). Dual-polarized antennas may also be used in MIMO systems. For example, a system with two dual-polarized antennas on each side of the link is equivalent to a 4x4 MIMO system. When it comes to deployment, the antennas may appear in different arrangements. For example, the antennas in a 4x4 MIMO system may be deployed in a square grid, along a line, or even in an L-shape if required. Often, physical site constraints dictate the deployment.

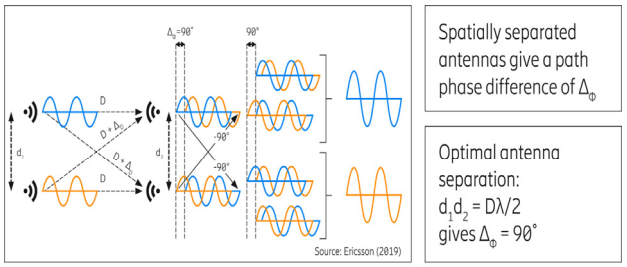

Principle of MIMO for microwave transmission where the spatially separated antennas gives a path length difference of Δ_Φ which corresponds to a phase difference of 90deg between the direct path and the cross path. By phase shifting by 90deg and summing the received signal, the two data streams are are restored perfectly and without any losses.

Figure 12. MIMO for microwave transmission – the principle

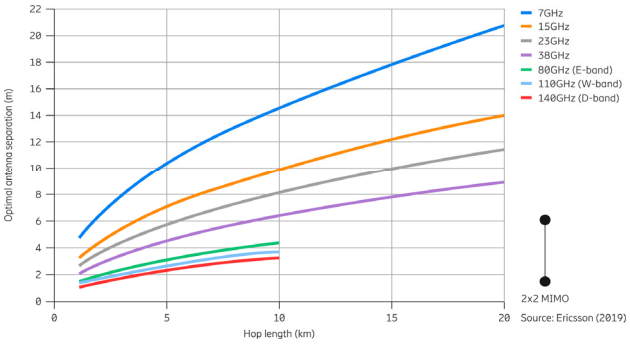

Figure 13. Optimal antenna separations for a 2x2 MIMO system

Figure 12 illustrates the principle of a 2x2 MIMO system, where a first transmit antenna is used to transmit a first signal data stream (blue), while a second transmit antenna (separated by a distance d1 from the first antenna) is used to transmit a second signal data stream (orange). Both signal data streams are received by two receiving antennas (separated by a distance d2) that are located at a distance D away from the transmitting antennas. Both signals are received by each one of the receiving antennas, which causes them to interfere with each other. However, it is possible to deploy the antennas in terms of separations d1 and d2 in such a way that there is an optimal phase shift ΔΦ of 90 degrees between the cross-channels relative to the direct channels. This means that by employing a proper interference cancellation scheme in the receiver, the interfering signals can be completely removed from the signals of interest. This can be done perfectly and without any performance loss if the ΔΦ corresponds to a 90 degree phase shift and, correspondingly, a ΔΦ of 90 degrees is said to be given by the optimal antenna separation. There are many antenna separations that give a ΔΦ of 90 degrees, but the optimal one is defined as the smallest separation, depending on the hop length D and wavelength λ (or frequency).

Figure 13 shows the optimal antenna separation in a 2x2 MIMO system for different frequencies versus hop length.

Higher frequency or shorter hop lengths allow for the use of smaller antenna separations, which makes the MIMO installation more compact. It should also be mentioned that it is possible to use sub-optimal antenna separations, as it may not be practical in some deployments to use the optimal antenna separation, due to it simply being

too large. The effect of sub-optimal antenna spacing is shown in Figure 14, where the MIMO capacity (spectral efficiency) is plotted against various degrees of sub-optimal antenna spacing for different MIMO antenna deployments. It shows how the capacity drops as the antennas become more sub-optimally spaced. However, even at 30 to 50 percent of optimal spacing, there is a huge capacity gain over a SISO system. The figure also shows that different antenna arrangements have different properties when the antennas are sub-optimally spaced. The square 4x4 MIMO deployment is more robust in comparison to sub-optimal spacing at the Signal-to-Noise Ratio (SNR) used in this example (the typical SNR of a microwave radio link).

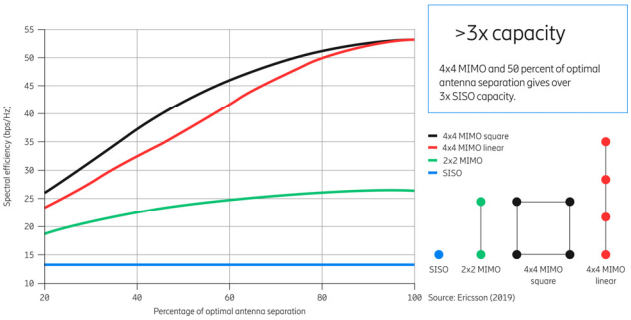

Figure 14. MIMO capacity depending on antenna arrangement

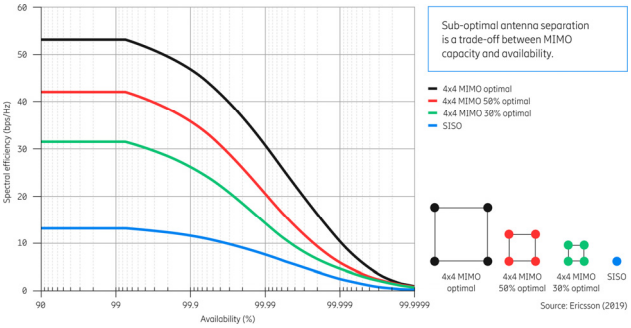

Figure 15. MIMO capacity and availability trade-off for sub-optimal antenna arrangements

In principle, the use of sub-optimal antenna separations will give a penalty in system gain, which in practice translates to a loss in availability. Figure 15 shows the effect of sub-optimal antenna separation in 4x4 MIMO systems deployed in square arrangements. It should be noted that the capacity drops when reducing the antenna spacing for fixed availability. Equally, it should also be noted that the availability will be lessened when reducing the antenna spacing for a fixed capacity. Therefore, the use of sub-optimal antenna spacing is a trade-off between MIMO capacity and availability.

A way to reduce the loss in capacity (or availability) when using sub-optimal antenna spacing is to use something called precoding. Precoding can be seen as a generalization of beamforming, where each data stream is transmitted over all (or a subset of) the antennas and with individual weighting (amplitude and phase) across the antennas. For example, the weighting can be chosen so that the Signal-to- Interference-and-Noise Ratio (SINR) of each data stream is maximized at the receiver side. Precoding will, therefore, put constraints on the phase synchronization of the radios in order to work properly. In MIMO systems without precoding, each individual data stream is transmitted from a single antenna, as depicted in the 2x2 MIMO system in Figure 12.

Optimizing MIMO for maximum effect

MIMO is a spectral-efficient multiple-antenna technology that can be used when the available spectrum is scarce or to enable >100Gbps in wide-band channels. The optimal antenna arrangement depends on the desired MIMO order, frequency and hop length. Sub-optimal antenna arrangements are possible, and sometimes even required, due to site installation constraints, but they will give a performance penalty in terms of reduced capacity and/or availability. Precoding over phase-synchronized transmitters can, to some extent, alleviate the penalty of using sub-optimally spaced antennas.

Breaking the 100Gbps barrier

Wireless backhaul's steady evolution over the last 40 years has been a response of continuous adaptation to the requirements of services enabled by new generations of mobile technology. The first commercial 100Mbps point-to-point links were available around the mid 90's; the first links supporting Gbps capacities emerged around 2010; and the first commercial links supporting 10Gbps recently became available. With this long-term trend in mind, point-to-point links supporting more than 100Gbps capacities are expected to be commercially available within the next 5-8 years. The key to increased capacity for previous backhaul generations has been accessing new frequency bands, wider channel bandwidths and higher modulation schemes. However, evolving along that path from today's 10Gbps links to 100Gbps would require a tenfold increase in channel bandwidth. This is not sustainable for large deployments of 100Gbps links, even with access to excessive spectrum beyond 100GHz. Due to this, new spectrum-efficient technologies such as line-of-sight MIMO will play a pivotal role in the commercialization of future ultra-high capacity point-to-point links. As described in the previous article on MIMO, this technology will multiply the spectrum efficiency, while maintaining or improving the system gain, enabling spectrum-efficient, high-capacity links over similar distances to today's backhaul links. To test MIMO in microwave fixed services, Deutsche Telekom and Ericsson jointly trialed a 100Gbps, 8x8 MIMO system using a single 2.5GHz channel in the E-band. The trial took place in April 2019 at the Deutsche Telekom Service Center in Athens, Greece.

Figure 16. A 100Gbps hop at OTE Academy in Athens, Greece, stretching over 1.5km towards OTE headquarters

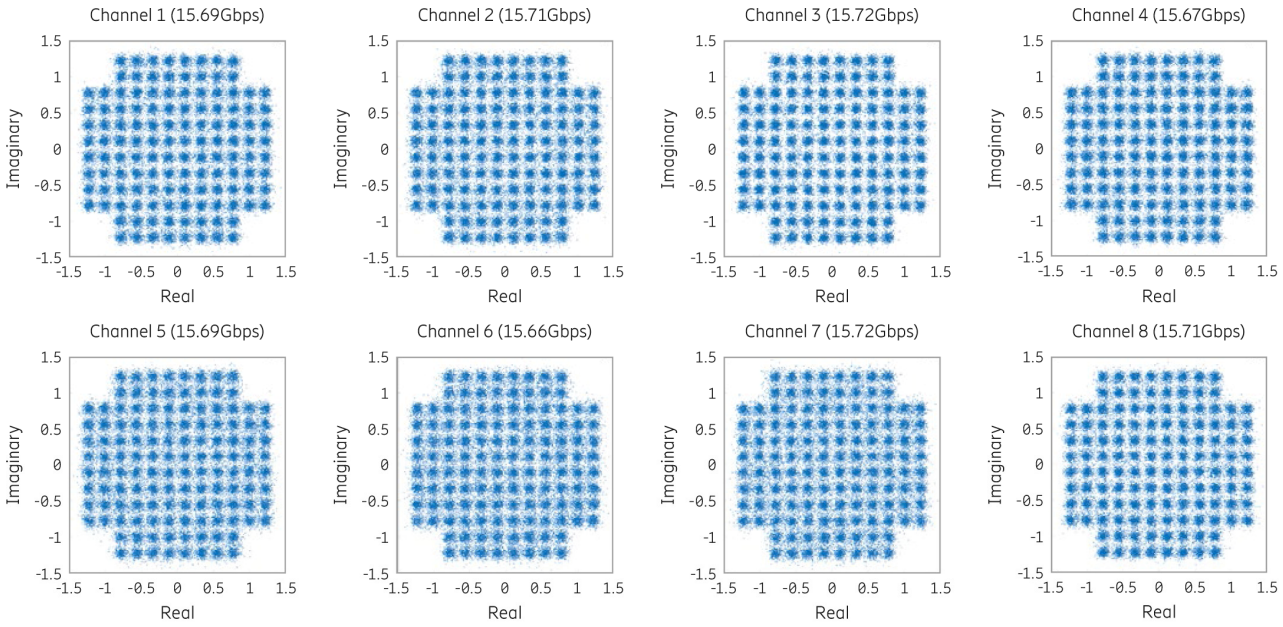

Example of throughput and constellation diagram per MIMO channel at 128QAM and 5dBm output power in a single 2.5GHz channel. Error-free throughput is 126Gbps.

Source: Ericsson and Deutsche Telekom (2019)

Figure 17. Measured throughput and constellation diagram per MIMO channel

A 1.5km link connecting the OTE headquarters (Hellenic Telecommunications Organization) in the Maroussi area with the OTE Academy (Figure 16) was used as the testbed. Four 0.6m parabolic reflector antennas were separated by 1.7m, which is the optimum antenna separation for a hop with a 73GHz carrier. Each antenna was deployed with two commercial Ericsson E-band radios in orthogonal polarization states. At the receiving end, the signals were received by a similar set of radios, recorded by a digitizer and evaluated offline.

The modulation scheme was changed from 64QAM to 128QAM and 256QAM, corresponding to a total bitrate of 105Gbps, 126Gbps and 139Gbps respectively in a 2.5GHz channel, and 84Gbps, 99Gbps and 113Gbps respectively in a 2GHz channel. The following experimental measurements were done in a 2.5GHz channel.

Figure 17 shows an example of the received constellation diagrams with 128QAM modulation, 5dBm transmitted power per radio and optimal antenna separation. The bit error rate for each channel is shown after error correction and the error-free throughput for all 8 channels combined is 126Gbps.

The left side of Figure 18 shows the antenna arrangement on the roof of OTE Academy, with the antennas arranged at optimum separation. The robustness of the antenna separation was tested by shifting the two lower antennas on one site towards the upper antenna row as shown in Figure 18 (right), first by 0.4m and then by 0.8m offset. Figure 19 shows measured throughput versus output power per radio for the three modulation formats. The power budget for 105Gbps throughput was higher than 25dB, resulting in a rain-limited availability better than 99.99 percent in Greece. This power budget would allow operation over long hop lengths with high availability in, for example, MBB configurations. Running a similar setup over a 7km hop would have resulted in 105Gbps capacity, with better than 99 percent availability.

The tolerance to reduced antenna separation is robust; a 0.8m offset results in availability estimated to be better than 99.99 percent for >100Gbps. A 135Gbps hop was reached with a power budget of 17.5dB, corresponding to availability of 99.97 percent.

The high throughput will result in a latency reduction. We expect a linear latency decrease with increased bitrate, resulting in a round-trip time below 5µs at 100Gbps. The radio units used in the trial were commercial, off-the-shelf E-band radios, further demonstrating the potential of this band. When moving to new frequency bands beyond 100GHz, more channels will be available to handle bandwidths in the order of a few GHz and, in fact, the optimum antenna separation between the antennas will decrease. For example, operating the same 1.5km hop on a W-band (110GHz) or a D-band (140GHz) carrier instead of an E-band carrier would result in an optimum antenna separation of 1.4m and 1.2m, respectively. The individual antenna sizes will be reduced for the same antenna directivity, leading to an overall reduction of the installation footprint. For short hops up to 500m, it will be possible to put all four antennas within one box, thus enabling single-box 100Gbps links. These high-frequency bands are therefore well-suited for future 100Gbps installations.

The work presented in this article shows the importance of applying spectral efficiency techniques, such as MIMO, on wireless backhaul. It demonstrates 100Gbps links with sub 5µs latency and telecom grade availability over hops measurable in kilometers with commercially available E-band radio technology. The need to process large amounts of high-speed data in parallel puts demanding requirements on cost and power consumption for the digital processors.

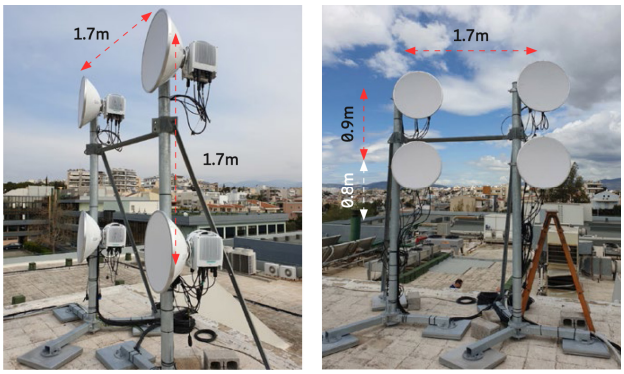

Figure 18. Antenna arrangement for the 100Gbps link at optimum antenna separation (left) and with 0.8m antenna offset (right)

We expect the first 100Gbps links to be deployed in 5 to 8 years, given the technology development in this field but also depending on the potential market demands. Market demand for increased capacity support continues to increase. Reaching 100Gbps and beyond is still far from today's capacity requirements in the access domain, which is typically in the order of 1Gbps, while ongoing capacity upgrades in advanced broadband networks are toward the 10Gbps milestone. However, in the aggregation networks (aka Edge/Core), capacity requirements are scaling from 10 to 100Gbps and this is most likely where we can initially expect these types of links.

These ultra-high capacity links will act as a cost and time-efficient compliment to fiber supporting ring closure, geographical redundancy in service provider networks or in private networks, such as campus and enterprise solutions. As a second phase, speeds in the pre-aggregation network segment and small cells fronthauling will drive up the last-mile capacities in multiples of 10/25Gbps.

The single-box 100Gbps links may be used for ultra-high capacity connections in dense urban areas inter-site distances of a few 100m. It is evident that microwave is well prepared for the network evolution of 5G and beyond.

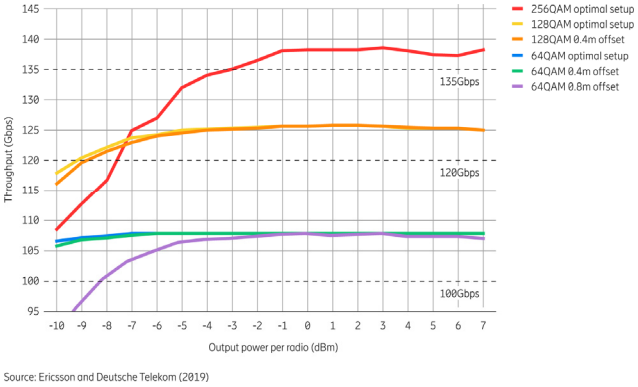

Source: Ericsson and Deutsche Telekom (2019)

Figure 19. Measured throughput versus transmitted output power per radio at optimal antenna setup and with 0.4m and 0.8m offset

Ericsson enables communications service providers to capture the full value of connectivity. The company's portfolio spans Networks, Digital Services, Managed Services, and Emerging Business and is designed to help our customers go digital, increase efficiency and find new revenue streams. Ericsson's investments in innovation have delivered the benefits of telephony and mobile broadband to billions of people around the world. The Ericsson stock is listed on Nasdaq Stockholm and on Nasdaq New York.

QUANTUM TECHNOLOGIES "MADE IN AUSTRIA" – AIT COORDINATES PILOT PROJECT OF EUROPEAN QUANTUM COMMUNICATION INITIATIVE (QCI)

21.04.2020, Austria. **AIT is Austria's center of expertise for quantum technologies, driving key initiatives to create a secure networked Europe.**

Magnus Brunner, State Secretary of the Austrian Federal Ministry for Climate Action, Environment, Energy, Mobility, Innovation and Technology (BMK), signed the EuroQCI Declaration on behalf of Austria in Brussels in late February 2020. In signing up to this European quantum communication infrastructure (QCI) initiative, 24 EU Member States have now confirmed their intention to create a European cybershield based on quantum communication infrastrucure within the next 10 years. The AIT Austrian Institute of Technology, Austria's largest applied research organisation, has been running the first European pilot project in the EuroQCI initiative – the Open European Quantum Key Distribution Testbed (OPENQKD) – since September 2019. The project is aimed at deploying quantum encryption to create a secure networked Europe. AIT expertise gained from many years of research will also play a key role in the first European QCI4EU study, which was launched in February 2020. This study aims to specify the user requirements and use cases which will drive development of the EuroQCI in close cooperation with the participating Member States. The findings will then be used to develop an overall system architecture for EuroQCI, composed of space-based and terrestrial solutions which are secure by design and will cover the entire European Union. The aim of EuroQCI is to facilitate the ultra-secure transmission and storage of information and data, and to link critical public communication assets throughout the entire European Union.

Over the past decade AIT has established an excellent international reputation as a quantum technologies specialist and coordinator of major European projects. They include the highly-competitive European Quantum Flagship programme aimed at developing quantum technologies for the mass market.

OPENQKD: quantum encryption for a secure networked Europe

In September 2019 the EU launched the EUR 15 million Horizon 2020 project OPENQKD. The findings of this 3-year project will flow directly into the EuroQCI initiative. The AIT-led consortium comprises 38 partners from 9 EU Member States, as well as the UK, Switzerland, Bosnia and Herzegovina, and Israel, consisting of manufacturers, network operators, system integrators, SMEs, research institutions, universities, certification and standardisation bodies, as well as end users, and together covering a broad range of expertise. Designed to establish a secure quantum communications network in Europe, as well as initiating a European ecosystem for quantum technology providers and application developers, the project will focus on developing a variety of demonstrators and future applications. They will include, amongst others, secure data transmission via telecommunication networks and appropriate storage in cloud infrastructures, the protection of sensitive medical information, official communication data, and the secure transmission of control signals used to operate critical infrastructure (telecommunication networks, energy supply). These activities are intended to protect Europe's digital data economy against present and future threats, such as those from quantum computers, and to secure Europe's strategic autonomy in the digital age. Further information: https://www.openqkd.eu

Quantum Flagship projects UNIQORN and CiVIQ

Launched in 2018 for a period of 10 years and with EUR 1 billion in funding, the Quantum Flagship programme is one of the European Commission's largest initiatives. Its goals include the development of a competitive European quantum technology industry, and establishing Europe as a dynamic and attractive region for quantum research.

The AIT-led project UNIQORN (Affordable Quantum Communication for Everyone: Revolutionizing the Quantum Ecosystem from Fabrication to Application) involves 17 partners from across Europe. It focuses on pioneering, user-focused research using photonic technologies to miniaturise quantum applications and create system-on-chip solutions. The aim is to optimise the costs of quantum technologies, making them available to the general public. Using specialised quantum-optical sources, miniaturised QKD transmission units and detector technologies on mainstream fabrication platforms, the project will provide important stimuli and breakthroughs, particularly for generating true random numbers, and thus for highly-secure key distribution. Further information: https://quantum-uniqorn.eu/aktuelle-news/

Research in the CiVIQ project focuses on the cost-efficient integration of quantum communication technologies in emerging optical telecommunication networks. A total of 21 partners, including leading telecom companies, integrators and QKD developers, are working to develop state-of-the-art flexible and cost-efficient systems for quantum key distribution (QKD), as well as novel quantum cryptography systems and protocols. In future, it should be possible to provide consumers, industry and institutions with innovative services which meet the needs of a secure telecommunications market. In this project, AIT is developing QKD prototypes and specialised software for field use. Further information: https://civiquantum.eu/

QUARTZ: quantum cryptography via satellite

Since 2018 AIT has played a significant role in a consortium coordinated by SES, the world's leading satellite operator, which is using quantum encryption to develop a satellite-based cybersecurity system. The QUARTZ (Quantum Cryptography Telecommunication System) project is supported by the European Space Agency (ESA). In addition to AIT and project coordinator SES, the QUARTZ consortium comprises a further 8 prestigious research institutions, universities and companies. Together, they will work until 2021 to design solutions for the distribution of secure keys between optical terrestrial ground stations, each connected to a quantum-enabled satellite via quantum links, and to develop the first software and hardware components this requires. Unlimited satellite coverage will help overcome the limits of today's fibre-based QKD systems, which are only able to transmit over a range of a few hundred kilometres, while also providing a globally available cybersecurity system, including networks in geographically dispersed areas.

Further information: https://www.ait.ac.at/quartz

Special note about data protection and privacy considerations at the AIT Austrian Institute of Technology

Protecting data and safeguarding privacy are essential in a modern society, and create the fundamental basis of trust upon which a society's cultural, social and economic development depends. Consequently, creating "security" is a core mission at the AIT Austrian Institute of Technology. In view of the many and constantly changing threats faced by our society, our task is to develop innovative approaches to combating these threats. For that reason, a particular focus of the research undertaken at AIT lies in methods, architectures and technologies which take privacy-by-design approaches in order to integrate the greatest possible level of data security into any technical solution. Data security and privacy are sensitive issues and must be protected, making them the primary consideration in all research activity undertaken at AIT.

POSTPONEMENT OF ITU DIGITAL WORLD 2020

ICTS IN THE COVID-19 CRISIS AND RISK OF A NEW DIGITAL DIVIDE

Geneva, 27 April 2020. **As a result of the ongoing COVID-19 crisis, the International Telecommunication Union (ITU) and the Ministry of Information and Communications, Viet Nam have taken the difficult decision to postpone ITU Digital World 2020, the global tech event for government, industry and SMEs. The event will now take place as ITU Digital World 2021 in September 2021 in the same venue in Ha Noi, Viet Nam. We believe this is the best and safest course of action to ensure the well-being and safety of all event participants and guarantee a successful event.**

The world is facing an unprecedented threat from COVID-19 and ICT has become a key ally in combatting this threat and helping to prevent, detect and diagnose disease. It has taken on a new importance in connecting us for health, work, education, entertainment, news, public announcements and to our friends and families. For the first time, digital solutions and platforms are being used on a massive scale to help cope with and respond to a pandemic.

The COVID-19 crisis has also, however, highlighted its own digital divide, where many families, workers, businesses and populations are not able to access or afford the benefits of digital technology. Action is urgently needed to ensure a fair access to ICTs, for the benefit of all. Now, more than ever, governments, industry, international organizations, NGOs, academia and other stakeholders must work together to find mutually beneficial solutions.

We must set ambitious, measurable goals for ensuring an equitable transition to the digital age. The SDGs offer an ideal framework for this, and ICTs themselves are essential tools for the achievement of these goals.

The Government of Viet Nam and ITU call upon global leaders, governments and the tech industry to ensure they are present and fully engaged, to rise to the challenge and strengthen the multilateral, collective digital response to this crisis. International events such as ITU Digital World 2021 are more important than ever as a platform bringing together the global ICT community to learn, share knowledge, debate and network.

We must work together to highlight the critical importance of ICT in the wake of COVID-19, address the stark inequalities of access and adopt concrete, urgent measures to accelerate digital transformation across all sectors and to connect all global citizens to digital services. Only by international cooperation and collaborative action will we be able to combat these types of threat, close the digital divide and build strong foundations for the future wellbeing of all.

EUROPEAN BROADCASTING UNION (EBU) RECOMMENDS MEASURES TO MITIGATE INTERNET CONGESTION

Geneva, 25 March 2020. **The EBU has issued a recommendation for public service media organizations to continue their efforts to avoid internet congestion and manage the potential impact of streaming media consumption during the COVID-19 pandemic. The full text of the EBU Technical Recommendation is available on the EBU T&I website.**

The Recommendation was approved by EBU Member representatives serving on the EBU's Technical Committee in conjunction with the members of the Digital Steering Committee. It suggests to temporarily cap streaming bitrates at appropriate levels for different end-user devices, particularly during day-time, and that public service media (PSM) organizations encourage audiences to consume their offerings over broadcast rather than broadband, and on fixed broadband rather than mobile, where possible. It also calls on EBU Members to take an active role in coordinating national efforts and to engage with other media, network operators and regulatory agencies to collectively analyse and respond to the situation.

"Public service media organizations are playing a key role in managing the crisis – not only by continuing to inform, educate and entertain, but also by actively engaging with all stakeholders to ensure that broadcast and broadband infrastructure is used in the most efficient way", said EBU Director of Technology & Innovation Antonio Arcidiacono.

Published as EBU R 149, the Technical Recommendation follows a call by the European Commission to help coordinate a European response to potential internet congestion issues that could be caused by stronger media consumption and the increased reliance on online collaboration tools during the COVID-19 crisis. PSM are the primary means of communicating with citizens in national emergencies. The EBU Technical Recommendation reaffirms the commitment of all EBU Members to their public service media obligations when weighing measures to reduce the impact of their services on the internet.

Recommends that during a time of crisis:

1) EBU Members, their local telecommunications network providers and administrations analyse the change in traffic patterns that may lead to Internet network congestion.

2) EBU Members act as facilitators at a national level for consensus amongst local OTT (overthe-top) providers in their efforts to address the challenges of Internet network congestion.

3) EBU Members seek to adapt their streaming services based on this analysis to address the challenge of network congestion while respecting their public service media obligations. Such measures could include:

a. Reducing the streaming bitrate by appropriate reduction of the top level of quality offered to clients particularly during office hours;

b. Arranging the adaptive streaming manifests to serve premium quality to fixed largescreen devices over mobile devices;

4) EBU Members might communicate with their audiences to adapt their viewing/listening patterns to help address the potential for network congestion. Where beneficial, measures could include informing their consumers to:

a. For linear services, favour the use of broadcast reception, via radio broadcast (FM, DAB/DAB+) and television broadcast DTT (Digital Terrestrial Television), DBS (Direct Broadcast Satellite) and Cable TV, which do not impact Internet network congestion;

b. At home, switch to WiFi/Internet where available rather than using 5G/4G/3G reception, as the former is more resilient to network congestion.

It is designed to provide guidelines to EBU Members and other broadcasters regarding adaptation of their streaming services and their audience's viewing and listening choices. The aim is to mitigate Interenet network congestion brought about by massive use of the internet for home networking and education purposes during the current COVID-19 pandemic. It is envisaged that this recommendation be updated as the crisis evolves.

Full text is available here: https://tech.ebu.ch/docs/r/r149.pdf

INNOVATIVE SOLUTION PROTECTS PEOPLE FROM THE CORONAVIRUS

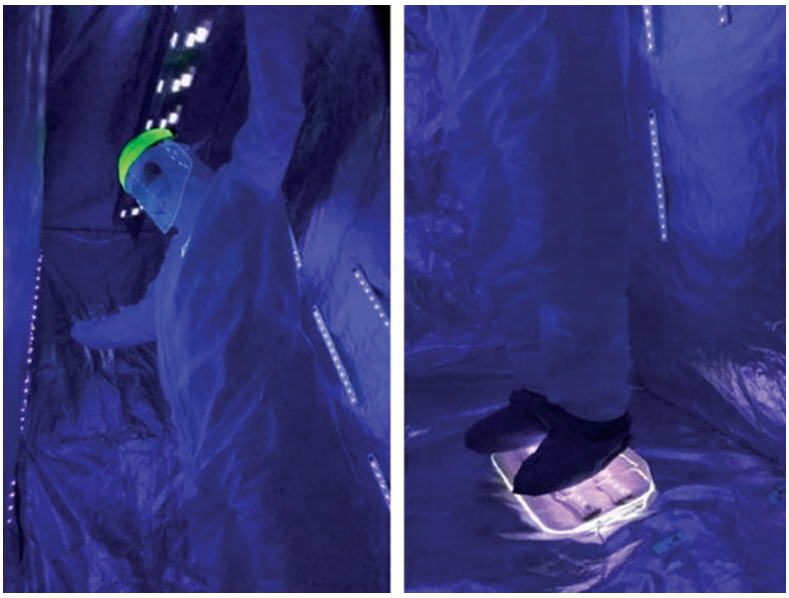

Olching, Germany, 20-03-17, LASER COMPONENTS GmbH. **Deep UVC LED arrays from Bolb, Inc. are helping to combat the coronavirus epidemic in the Chinese metropolis of Wuhan. Emitter arrays with a power output of between 1.2 W and 2.5 W emit strongly disinfecting UVC light that kills not only antibiotic-resistant germs such as MRSA but also dangerous viruses such as the coronavirus (SARS-CoV-2).**

In the newly built Huoshenshan Hospital, this technology is already being used to decontaminate doctors and nursing staff when they enter or leave the corona isolation ward in their infectious disease protective clothing. To do this, doctors and nursing staff simply have to be irradiated from all sides with highly efficient UVC light for around 30 seconds.

The wavelength is selected in such a way that it changes the RNA of the viruses in a short amount of time so that they no longer pose a threat. Since the epidemic suit also protects against UVC radiation, there is no danger to humans. To make the invisible UVC radiation visible, the headpiece of the protective equipment is coated with a fluorescent paint that glows as soon as the emitters are activated.

Germicidal LEDs (G-LEDs) from the US manufacturer Bolb are available from LASER COMPONENTS in Europe and the USA. In addition to use in hospitals and biomedical applications, UVC modules enable mobile and on-site solutions for treating drinking water, for example. In agriculture and horticulture, this technology can replace chemical pesticides and thus promote cost-effective, environmentally friendly forms of cultivation. UVC emitters can also be used in refrigerators to increase the shelf life of food.

Bolb Inc has introduced a powerful germicidal photonic platform based on their proprietary patented technical breakthrough - Germicidal LED (GLED), which is considered the world's best performing deep ultra-violet (DUV) LED and is capable of delivering a 10x performance improvement compared to current state of the art devices. These devices will have a dramatic impact on the worldwide disinfection and pathogen destruction industries enabling a new wave of solutions in critical market segments, such as Water Treatment, HAI Prevention, and Horticulture and Food Safety. By replacing mercury-based germicidal lamps with LEDS, Bolb opens up new applications of light-based pathogen destruction for surface, water, and air treatment, whenever form factor, upfront and operations costs, energy efficiency, convenience, and workflow considerations demand flexible and tailored photonic configurations.

To meet customer specifications quickly and flexibly, LASER COMPONENTS opened its own electronics production facility. At this facility, circuit boards are designed to drive PLDs and APDs. We also manufacture prototypes before they go into series production. Another major field is the individual production of customer-specific products!

Production Steps. *Our customers state their electronics requirements, and our R&D engineers create an appropriate CAD design. This software directly controls the circuit board milling machine for the production of prototypes. Electronic components are applied manually during this developmental stage. The results of a comprehensive inspection of these prototypes determine whether they proceed to series production.*

PLD Modules. *One example of a series product is our PLD modules. With these modules pulsed laser diodes can be operated safely, resulting in an optimal and thus reliable driver. The PLD is already integrated into the module. One unique product is our adjustable modules, which allow the continuous adjustment of both the output power and pulse length. They are particularly well suited for product R&D to test the ideal settings.*

High Voltage Modules for the Operation of APDs. *Temperature-stabilized high voltage modules are particularly well suited for the operation of Avalanche photodiodes (APDs). Output voltage and temperature compensation can both be matched exactly to the APD being used. Connecting the module and the APD is simple, and can be done with the help of the supplied diagram.*

APD Modules. *The APD modules are based on low-noise avalanche photodiodes made of either silicon or InGaAs with a built-in preamplifier and high voltage supply. A temperature compensation function allows the APD to be operated at constant gain across a wide operating temperature range.*